Task Leaders Meeting (IEA)

Capri, September 14-18, 2008

Task 2.4 F

Experimental and numerical study of the structure of a stoichiometric ethanol flame

N. Leplat and J. Vandooren

CSTR. Laboratoire de Physico-Chimie de la Combustion
Université catholique de Louvain
Place Louis Pasteur, n°1
1348 Louvain-la-Neuve. Belgique

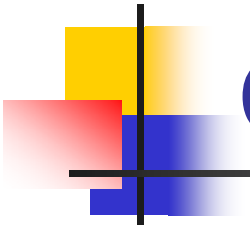

Outline

1. Introduction
2. Experimental results
3. Conclusion

Utilisation of ethanol

- Advantage → Low impact on the environment :

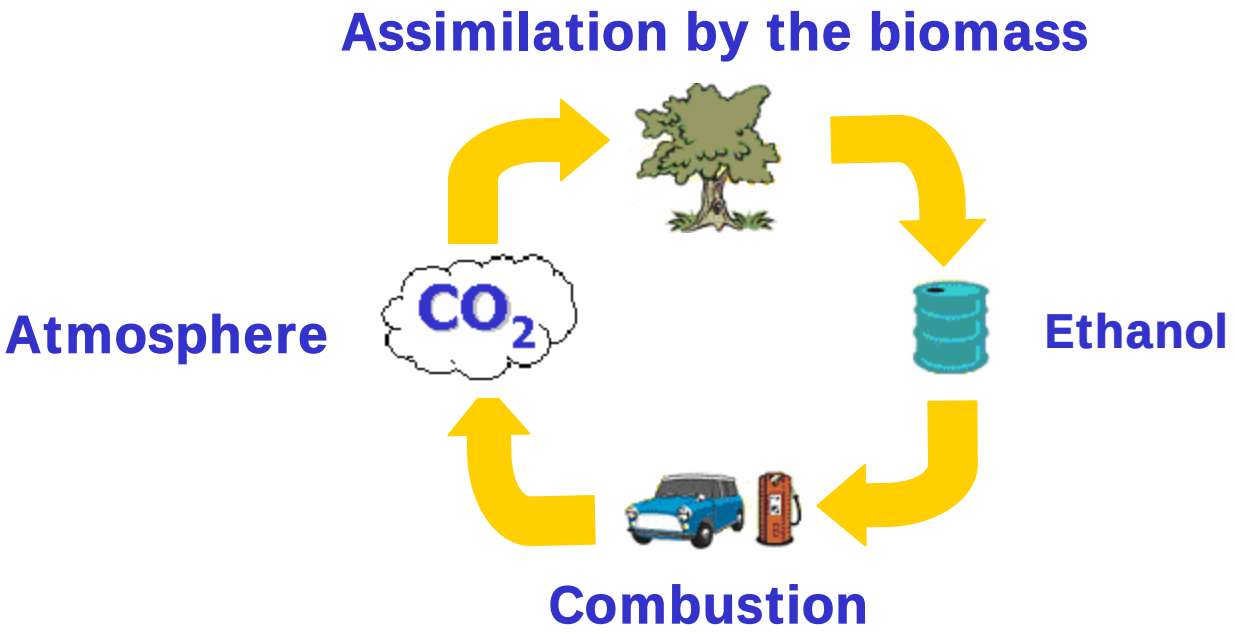

- **Disadvantage** → Hight cost of the production

Aim of this work

- Study the structure of a premixed ethanol flame
- Direct comparison :

Experimental results ⟷ Numerical results

$X C_2H_5OH$	$X O_2$	$X Ar$	ϕ	V_0	W.P.
0.0687	0.2059	0.7254	1	46.42	50

ϕ : equivalence ratio V_0 : initial flow velocity (cm/s) W.P. : Working pressure (mbar)

- Modelling with the PREMIX program :

R. Kee, F.M. Rupley, J.A. Miller, Sandia Report, SAND89-8009B.UC-706, 1993

Experimental setup

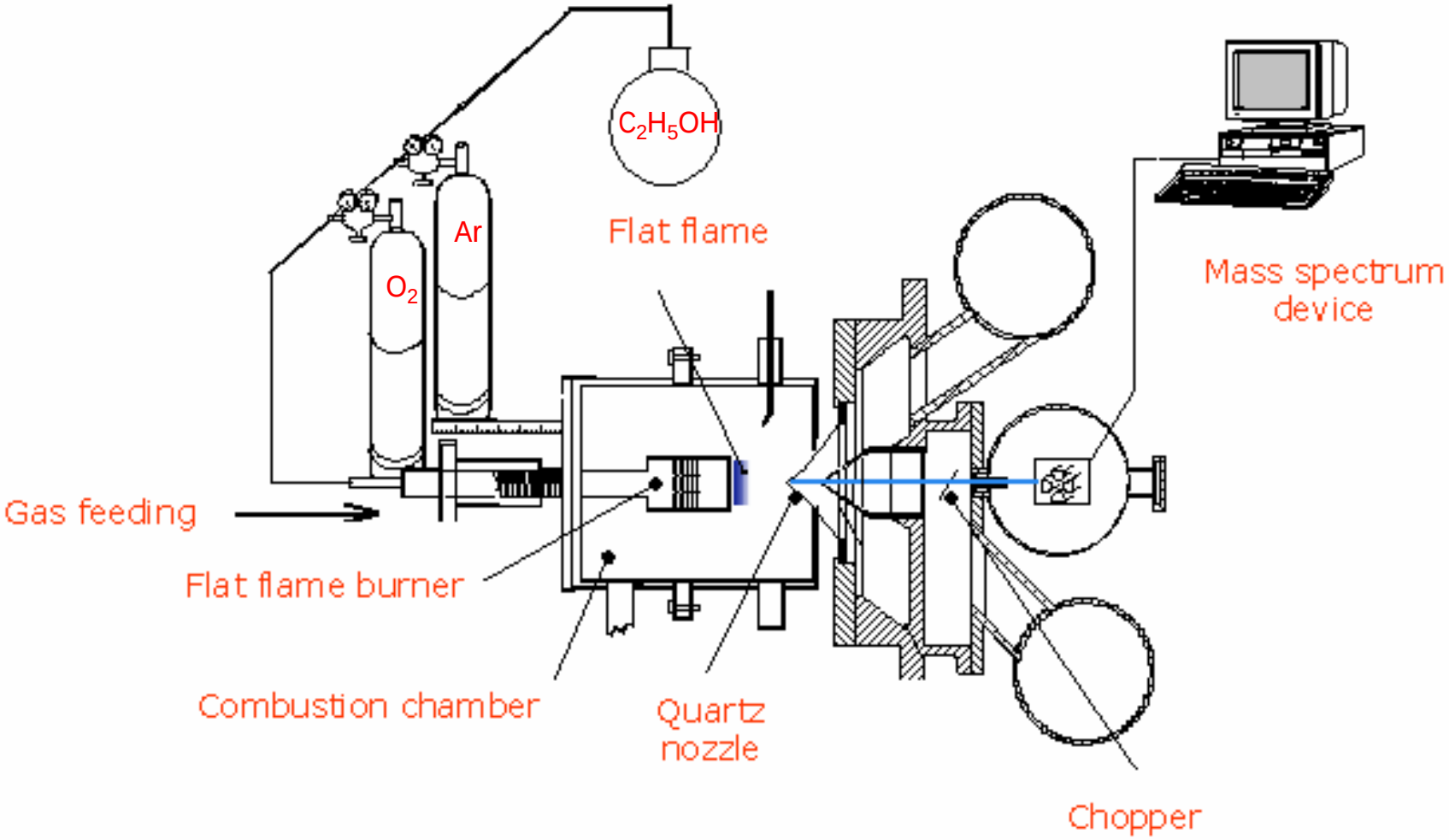

Mole fraction profiles of main chemical species

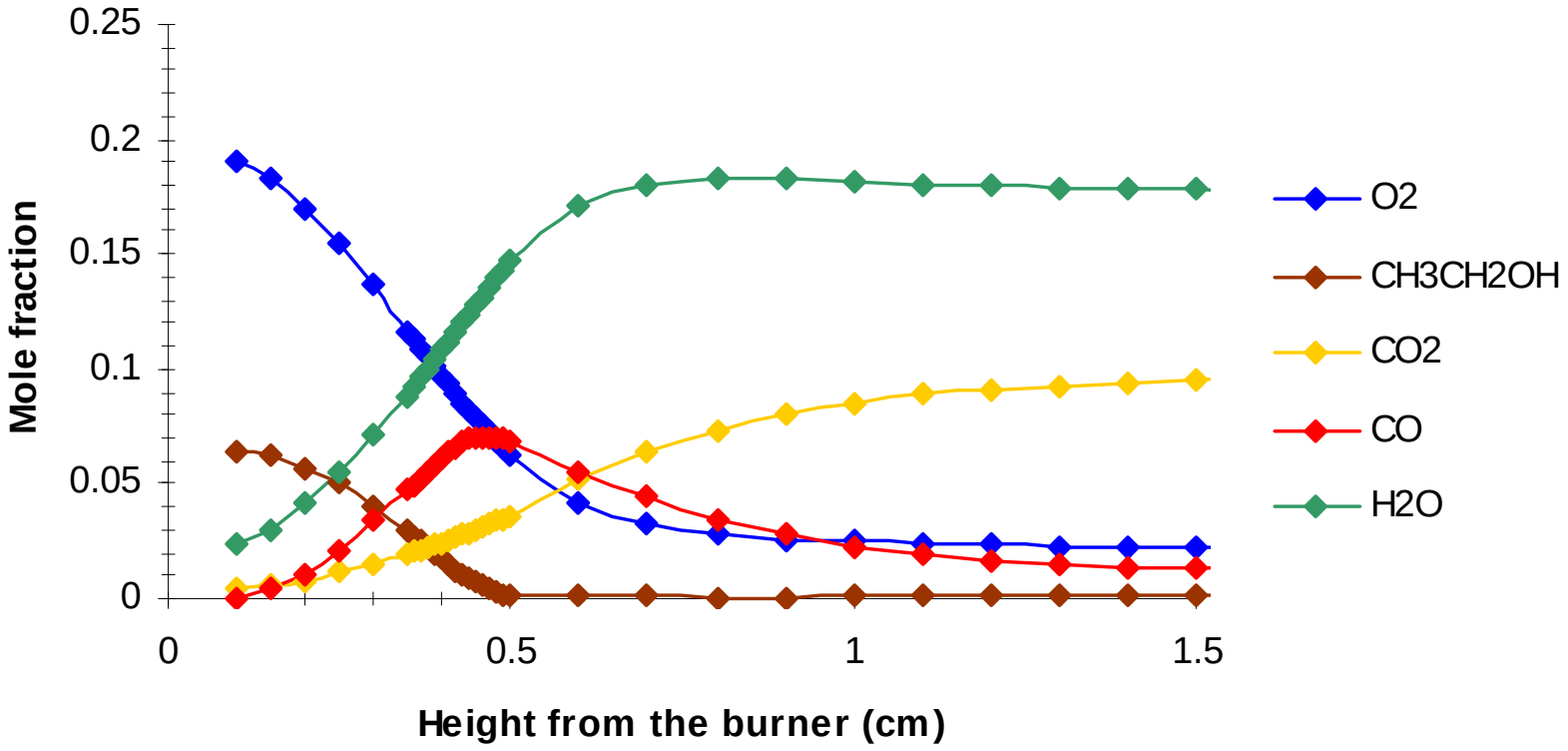

The studied kinetic mechanisms

Name	Number of reactions	Number of species	Efficiency of a third species
Dunphy	97	29	No
M. P. Dunphy, P. M. Patterson et J. M. Simmie, Journal of the Chemical Society Faraday Transactions, volume 87, 1991			
Norton	278	32	Yes
T. S. Norton et F. L. Dryer, International Journal of Chemical Kinetics, Volume 24, 1992			
Dagaut	76	25	No
P. Dagaut, J. C. Boettner et M. Cathonnet, Journal de Chimie Physique et de Physico-Chimie Biologique, volume 89, 1992			
Marinov	383	55	Yes
N. M. Marinov, International Journal of Chemical Kinetics, Volume 31, 1999			

Ethanol

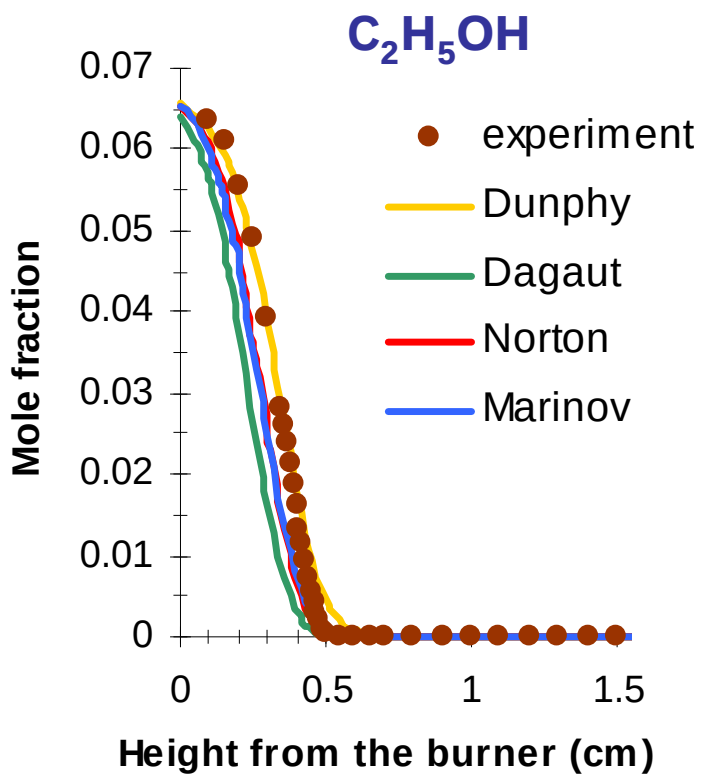

Ethanol consumption main pathways :

- **$CH_3CH_2OH + X = CH_3CHOH + XH$**

Where X is the radical H or OH or O

Norton	**5,2 %**	**44,1 %**	
Marinov	**20,1 %**	**12,3 %**	**5,0 %**

- **$CH_3CH_2OH + X = CH_3CH_2O + XH$**

Where X is the radical H or OH or O

Norton		**17,5 %**	
Marinov	**7,4 %**	**32,3 %**	**1,8 %**

- **$CH_3CH_2OH + X = CH_2CH_2OH + XH$**

Where X is the radical H or OH or O

Norton		**26,5 %**	
Marinov	**11,5 %**	**8,8 %**	**0,8 %**

- **$CH_3CH_2OH = CH_3 + CH_2OH$**

Norton	**6,8 %**

Carbon monoxyde

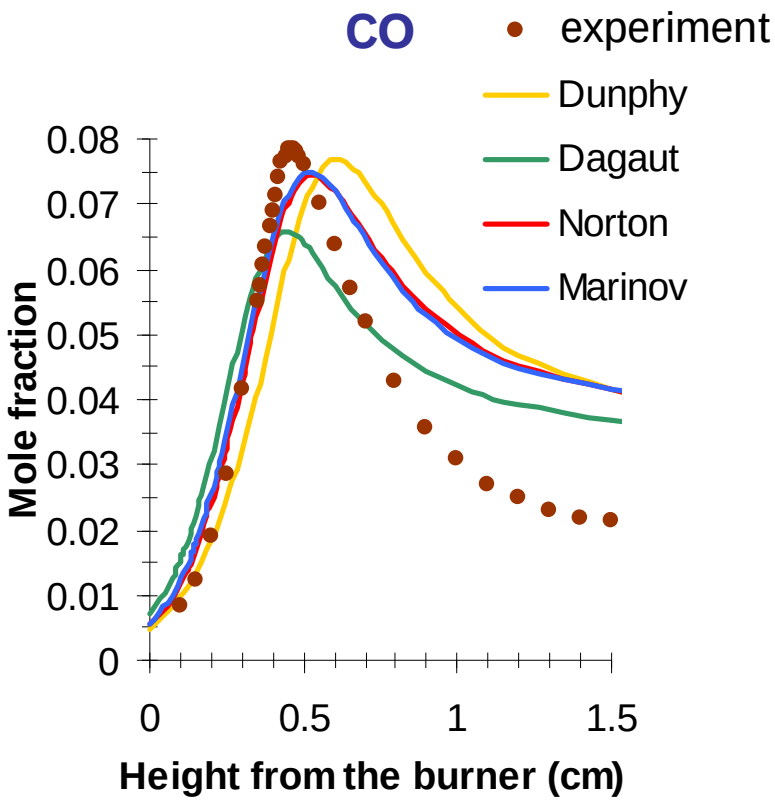

CO Formation main pathways :

- **HCO + X = CO + XH**

Where X is H or OH or O or O_2 or M

Norton 13,2% 22,8% 21,8%

Marinov 16,6% 14,0% 1,8% 36,8% 21,4%

- **$CH_3CO + M = CO + CH_3 + M$**

Norton 42,1%

- **$CH_2 + X = CO + (X - O)H_2$**

Where X is O or O_2

Marinov 6,9% 2,4%

Carbon dioxyde

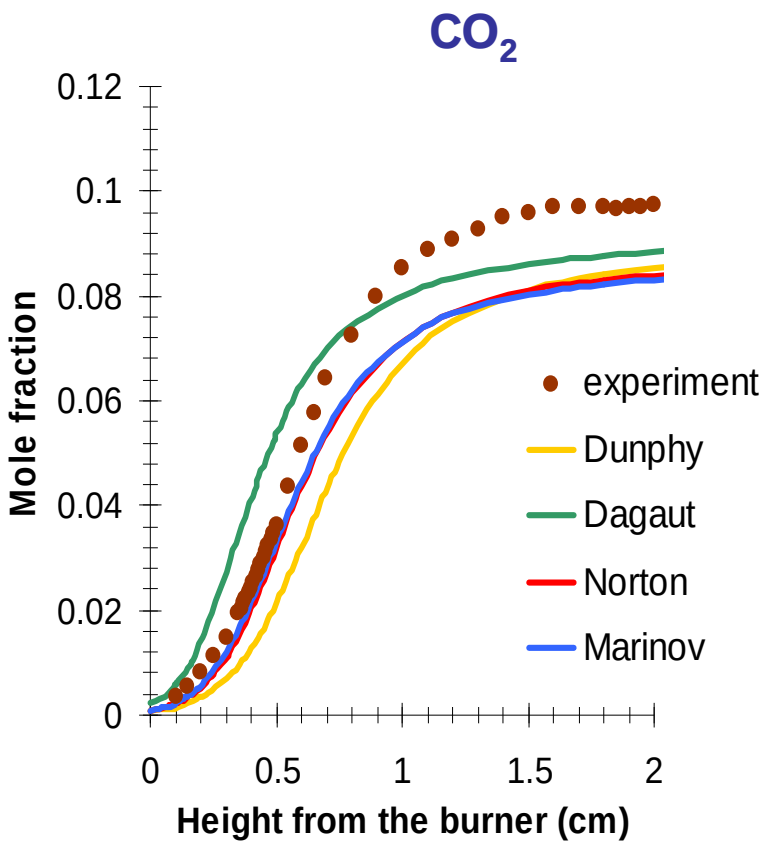

CO_2 Formation main pathway :

- Only one reaction :

$CO + OH = CO_2 + H$ ➡ 100%!

Remark :

- The CO simulated mole fraction profiles are too high
- The CO_2 simulated mole fraction profiles are too low

Conclusion

- We must increase the reaction rate of the precedent reaction

H_2 and O_2

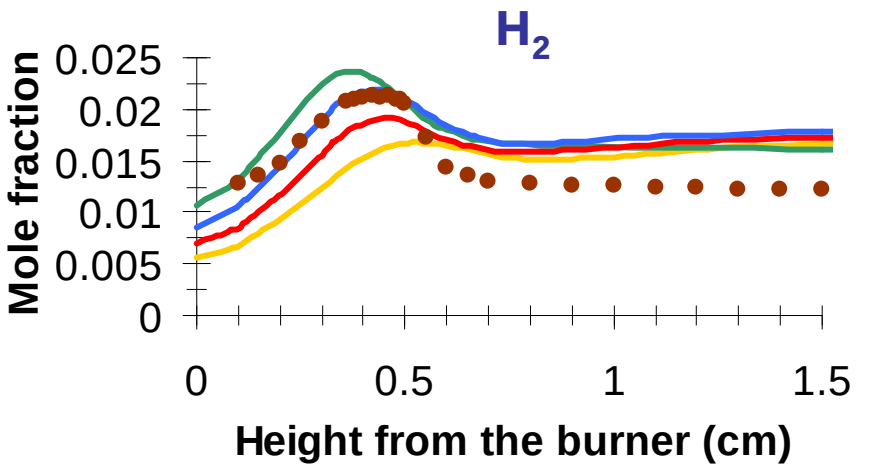

- Good position of the maximum of mole fraction with Norton and Marinov
- Good simulated mole fraction values until 0,5 cm with Marinov
- But overestimation of simulations in the post combustion zone

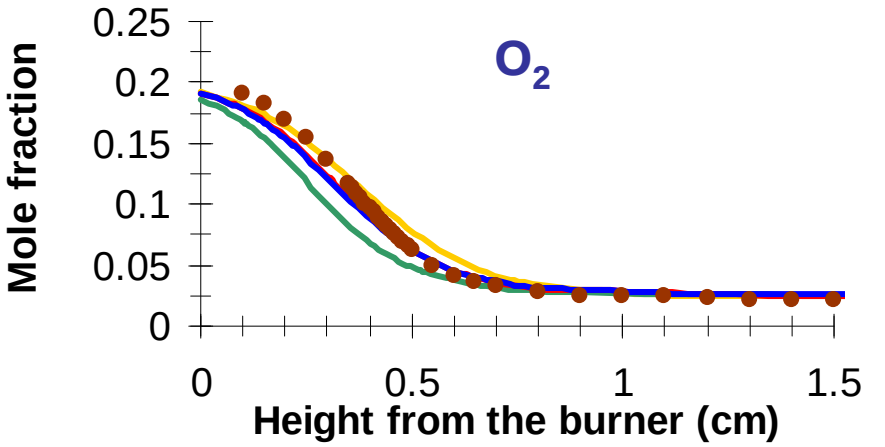

- The experimental profile is very well predicted with the mechanisms of Dunphy, Norton and Marinov
- Modelled consumption is too fast with the mechanism of Dagaut

H_2O and OH

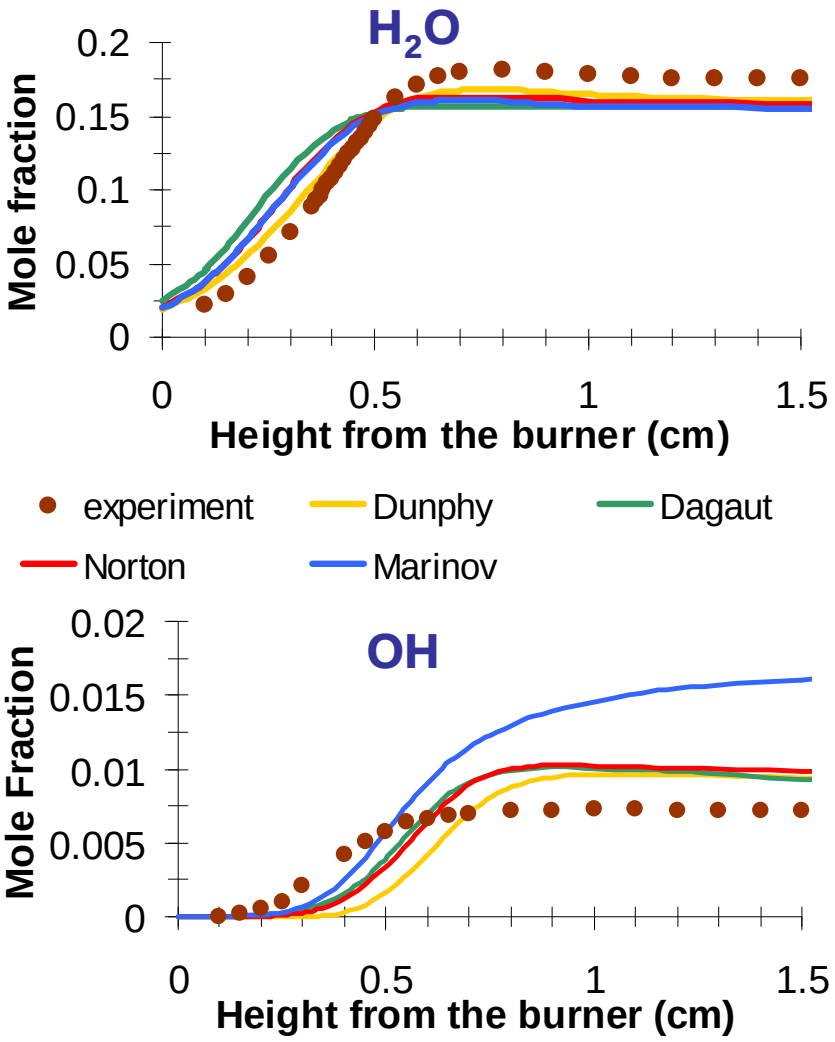

- The experimental profile is well simulated with the mechanism of Dunphy
- Modelled formations are shifted towards the fresh gases region with the mechanism of Dagaut, Norton and Marinov
- The calculated mole fraction values in the burned gases are underestimated
- Simulated formations are too low in the flame front
- In the burned gases, the calculated mole fraction values are too high,
  $\Rightarrow$ especially Marinov

CH_3 and CH_4

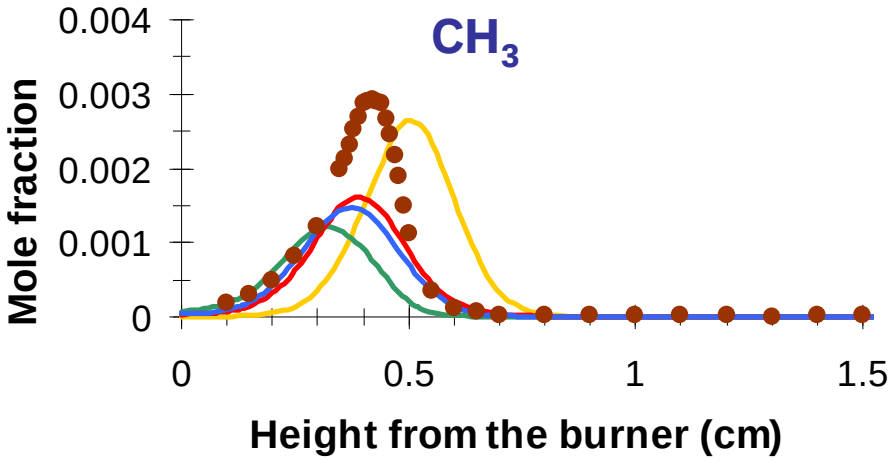

- Position of mole fraction is well simulated with the mechanisms of Norton and Marinov
- The mole fraction values are underestimated by mechanisms

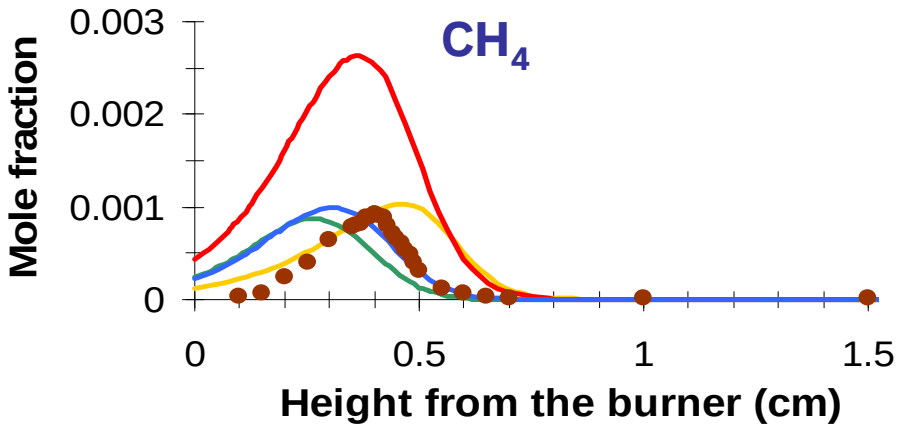

- Maximum mole fractions are well simulated with the mechanisms of Dagaut, Dunphy and Marinov
- The position of the maximum does not match, except with Norton

C_2H_4 and C_2H_2

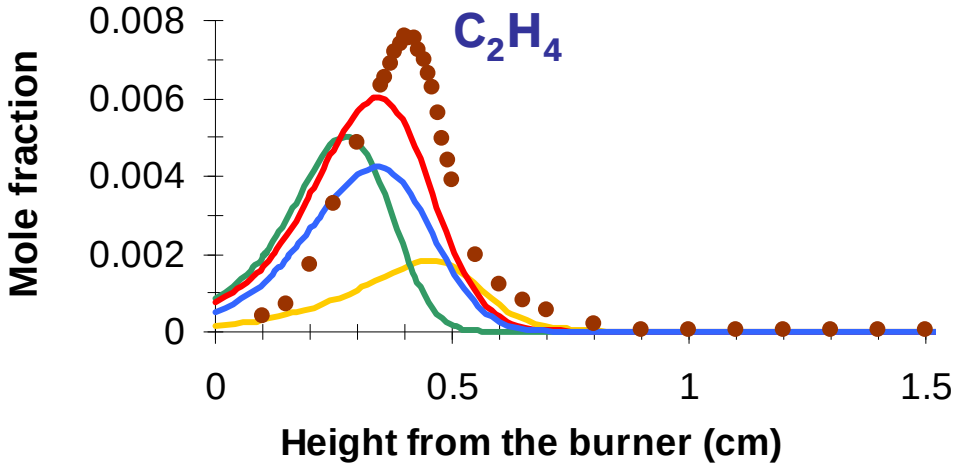

- The position of the calculated maximum is well simulated with the Norton's and the Marinov's mechanisms
- The simulated mole fraction values are underestimated

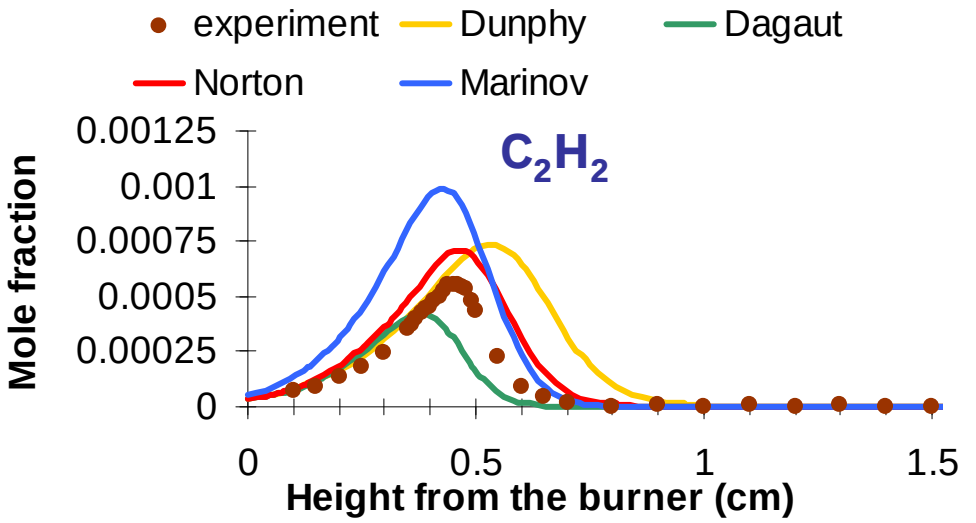

- The experimental profile is very well simulated with the mechanism of Norton
- The acetylene formation is too fast and early with the Marinov model

CH_3HCO and Ar

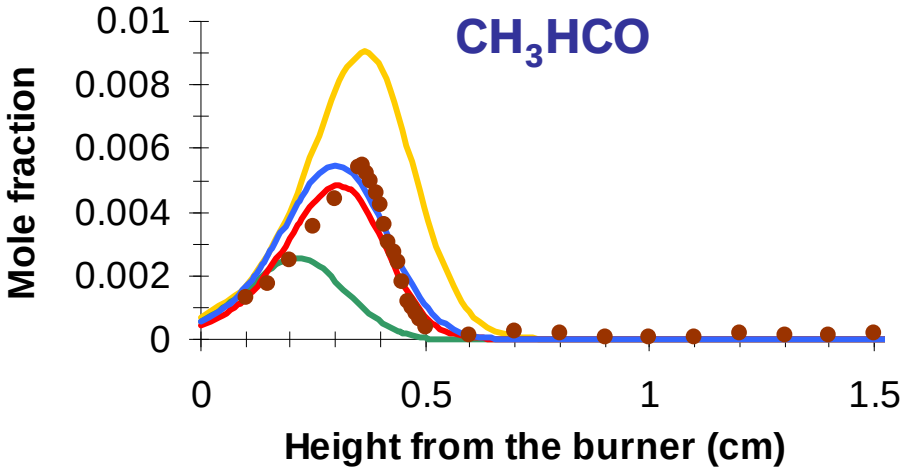

- The experimental profile is very well simulated by the mechanisms of Norton and Marinov
- The position and the maximum mole fraction values disagree with the mechanisms of Dunphy and Dagaut

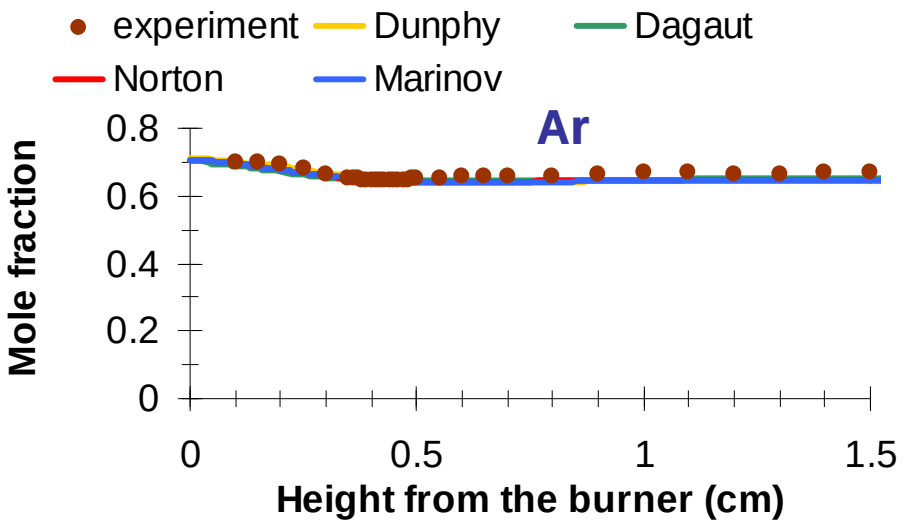

- The experimental profile is well simulated by all mechanisms
- Argon does not allow us to establish the validity of a mechanism in flames

Conclusion about the mechanisms

Mechanism of Dunphy :

- Good agreement for the mole fraction profiles of C_2H_5OH, O_2 and Ar
- The profile positions are generally shifted towards burned gases compared to experimental profiles
- The mole fraction values are not well predicted for H_2, C_2H_2, C_2H_4, CH_3HCO, CO and CO_2

Mechanism of Dagaut :

- Good agreement for the mole fraction profiles of C_2H_5OH, O_2 and Ar
- The profile positions are generally shifted towards fresh gases compared to experimental profiles
- The mole fraction values of intermediate species and products are systematically smaller than the experiment. (except for CH_4)

Cannot be validated by the structure of this ethanol flame (ϕ=1)

Conclusion about the mechanisms

Mechanism of Norton :

- Good agreement for the mole fraction profiles of C_2H_5OH, O_2, Ar, CH_3HCO and C_2H_2
- The positions of the maximum are always well predicted
- The mole fraction values of some profiles are not well predicted : especially for CH_3 and CH_4

Mechanism of Marinov :

- Good agreement for the mole fraction profiles of C_2H_5OH, O_2, Ar and CH_3HCO.
- The profile positions are generally well predicted
- The mole fraction values of some species are not well predicted : OH, C_2H_2, C_2H_4 and CH_3

Best agreement is observed with these mechanisms.
But, the reaction pathways show significant differences between these mechanisms

Common reaction pathways of ethanol consumption

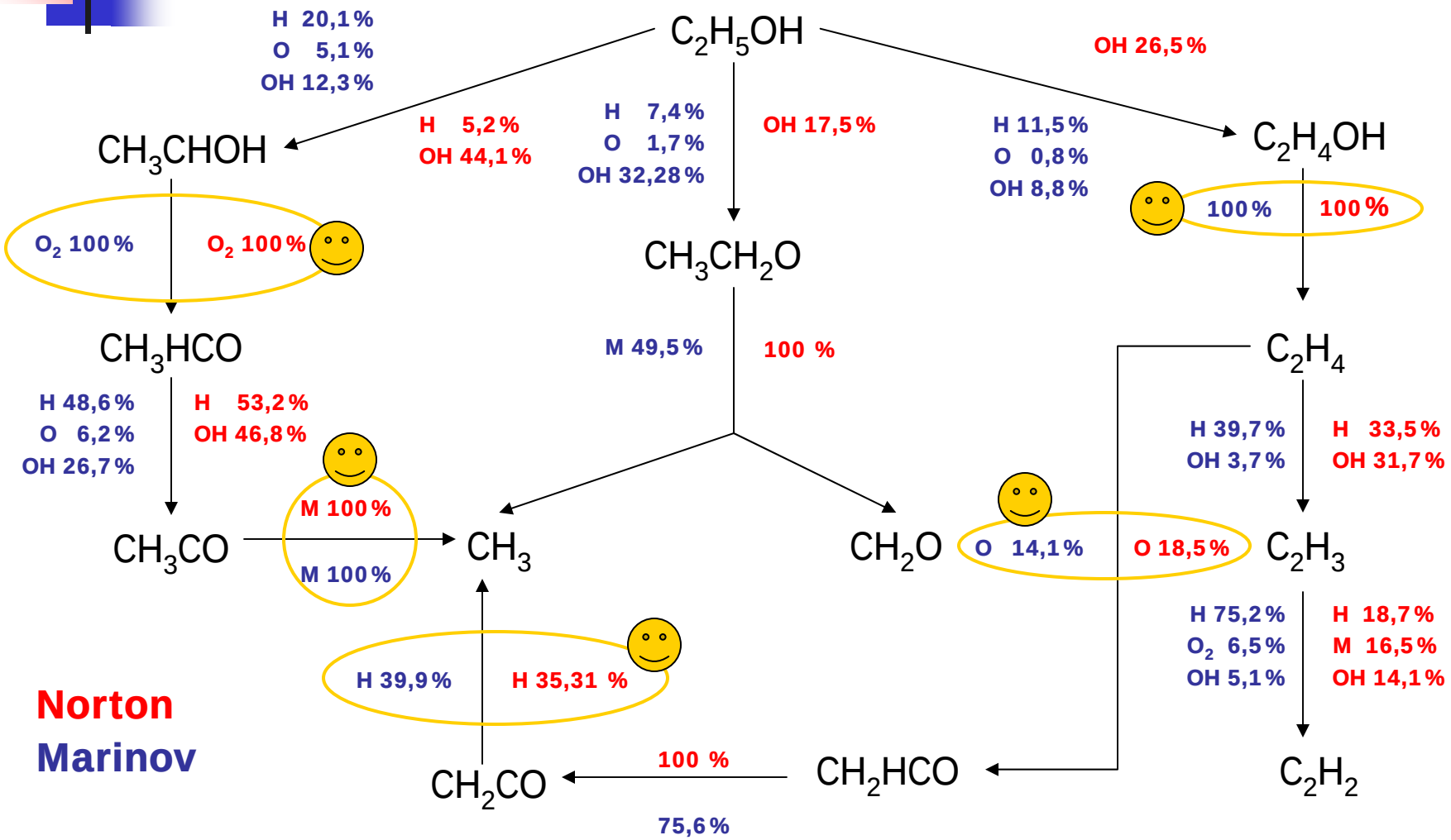

Common reaction pathways of CO_2 formation

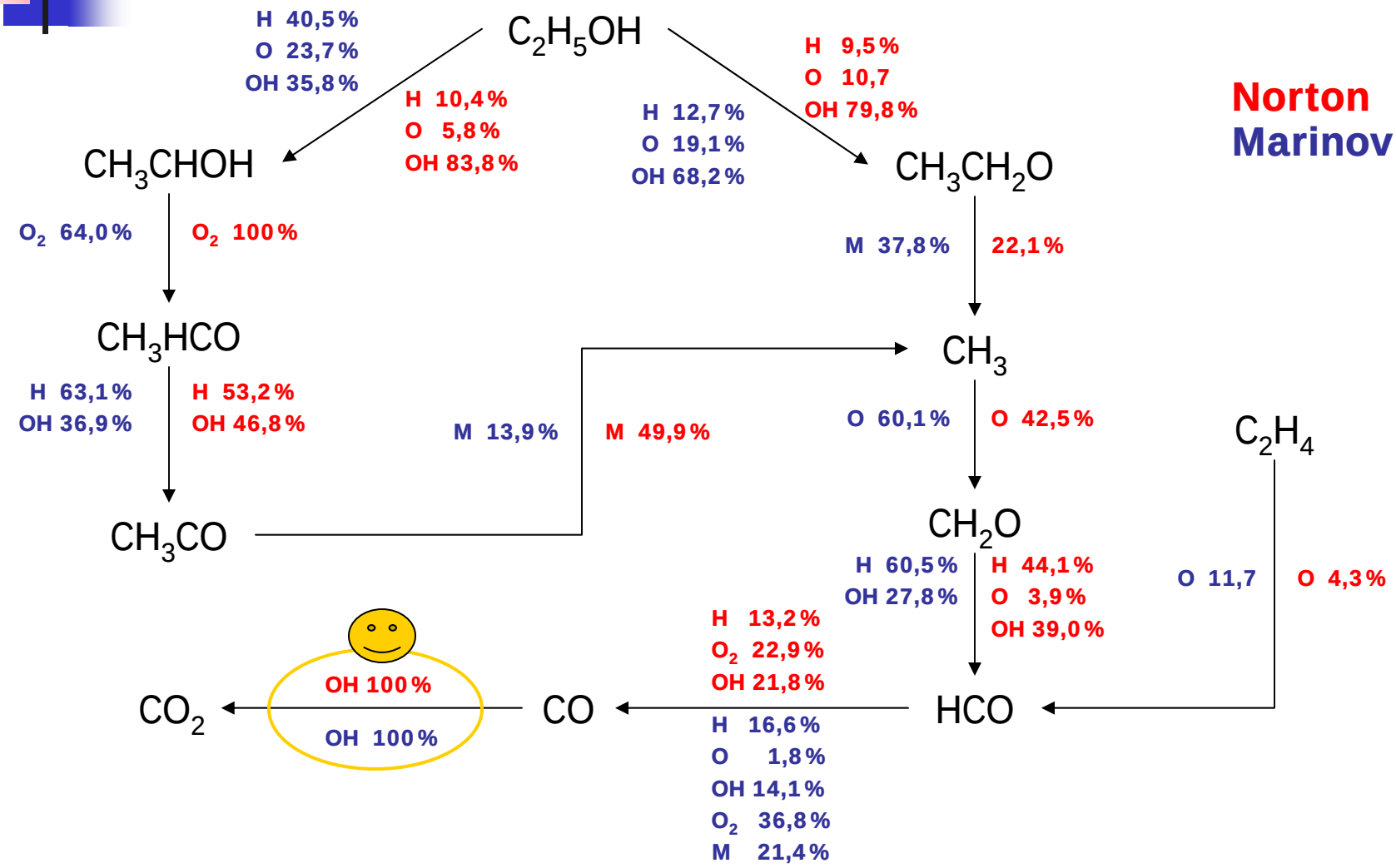

Norton
Marinov

Final conclusion

- A better mechanism should be built
- This new mechanism should be mainly based on the mechanisms of Norton and Marinov
- New experiments must be performed to validate this new mechanism :
  - by measuring mole fraction profiles of other chemical species
  - by checking the validity with various initial conditions like working pressure, equivalence ratio,...

Acknowledgments

Dr. V. Dias

C. Duynslaegher

C. Smets

V. Detilleux

C. Renard

P.J. Van Tiggelen

The authors are grateful to the Ministère de la Région Wallonne for the financial support

Temperature profile : Thermocouple

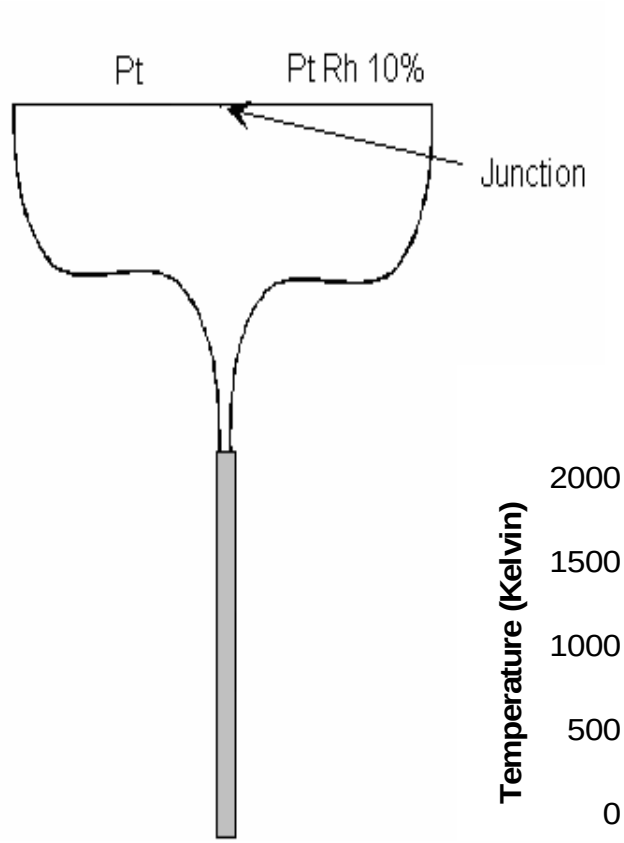

- The potential (mv) at the junction of the two alloys depends on the temperature
- An appropriate function will correlate the voltage with the temperature

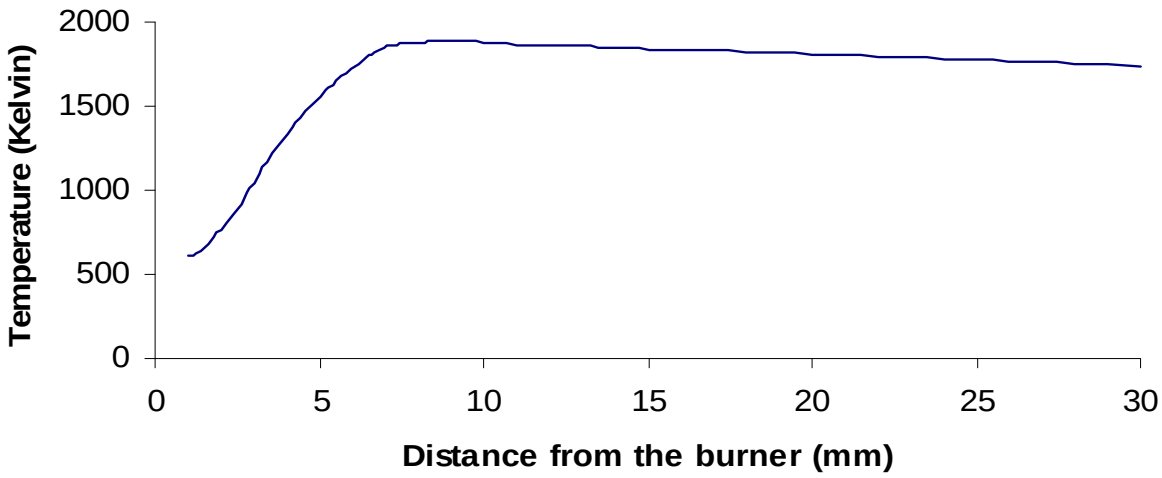

Conversion into mole fraction profiles

- Calibration of each chemical species with an appropriate cool gas mixture wich composition close to these in the flame
  $S_i = X_i / I_i$ -> sensibility factor (s_i)
- Solution of a multiple equation system:

$$\left(X_i\right)_{flame} = \left(\frac{S_j}{S_i}\right)_{mixture} \left(\frac{I_i}{I_j}\right)_{flame} \left(X_j\right)_{flame}$$

j = reference chemical species
i = the other species

$$\sum_i X_i = 1$$

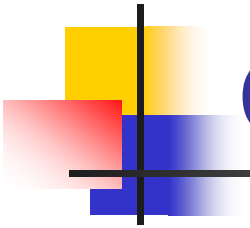

Outline

1. Introduction
2. Experimental results
3. Conclusion

Utilisation of ethanol

- Advantage → Low impact on the environment :

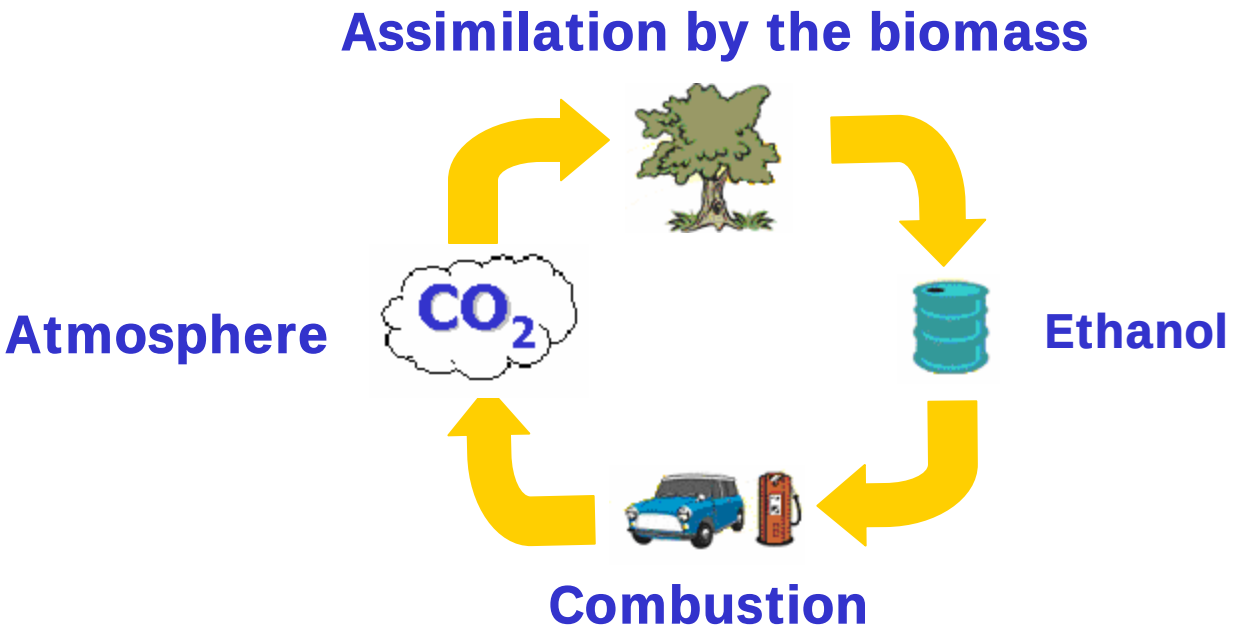

- **Disadvantage** → Hight cost of the production

Aim of this work

- Study the structure of a premixed ethanol flame
- Direct comparison :

Experimental results ⟷ Numerical results

$X C_2H_5OH$	$X O_2$	$X Ar$	ϕ	V_0	W.P.
0.0687	0.2059	0.7254	1	46.42	50

ϕ : equivalence ratio V_0 : initial flow velocity (cm/s) W.P. : Working pressure (mbar)

- Modelling with the PREMIX program :

R. Kee, F.M. Rupley, J.A. Miller, Sandia Report, SAND89-8009B.UC-706, 1993

Experimental setup

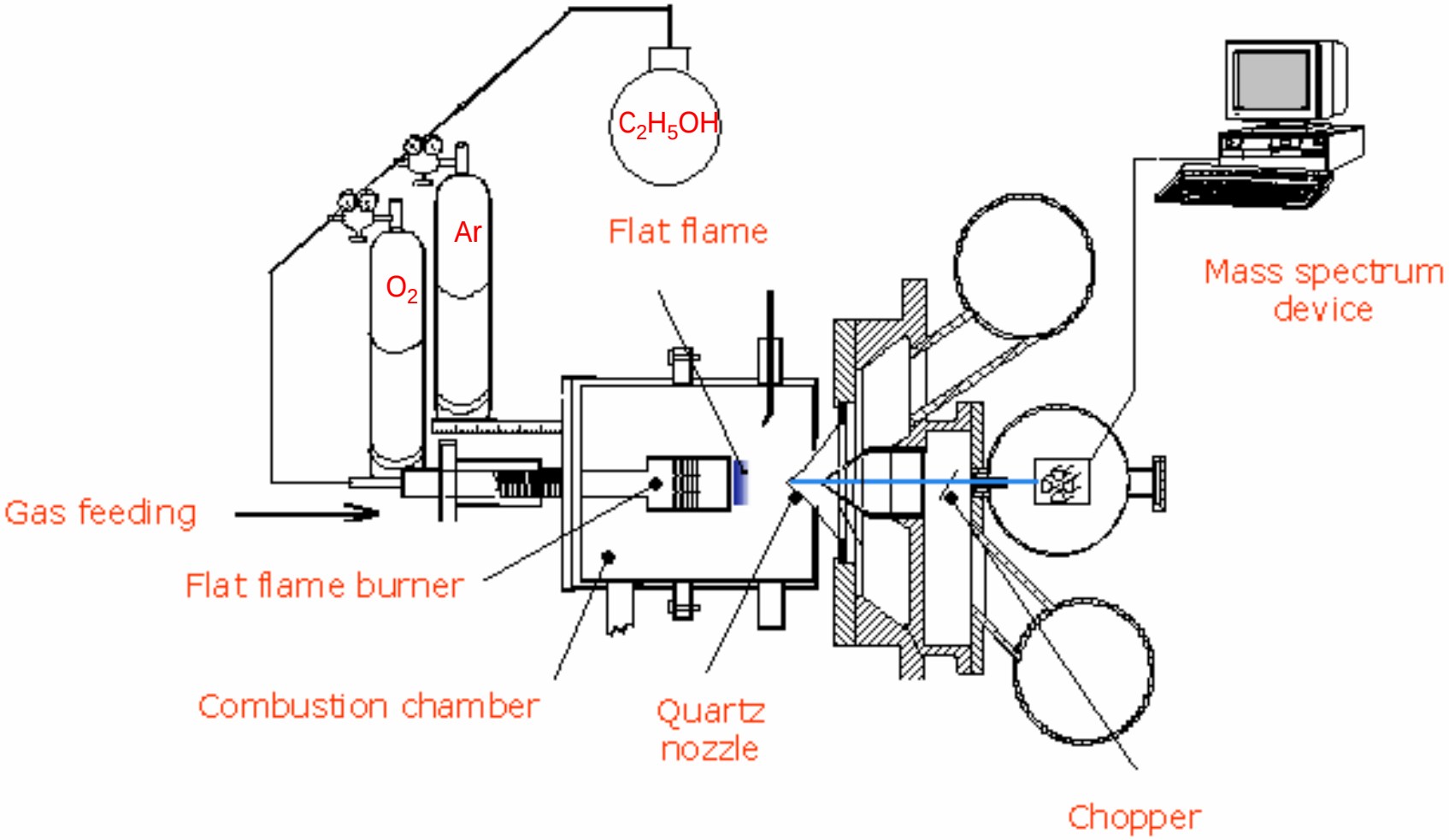

Mole fraction profiles of main chemical species

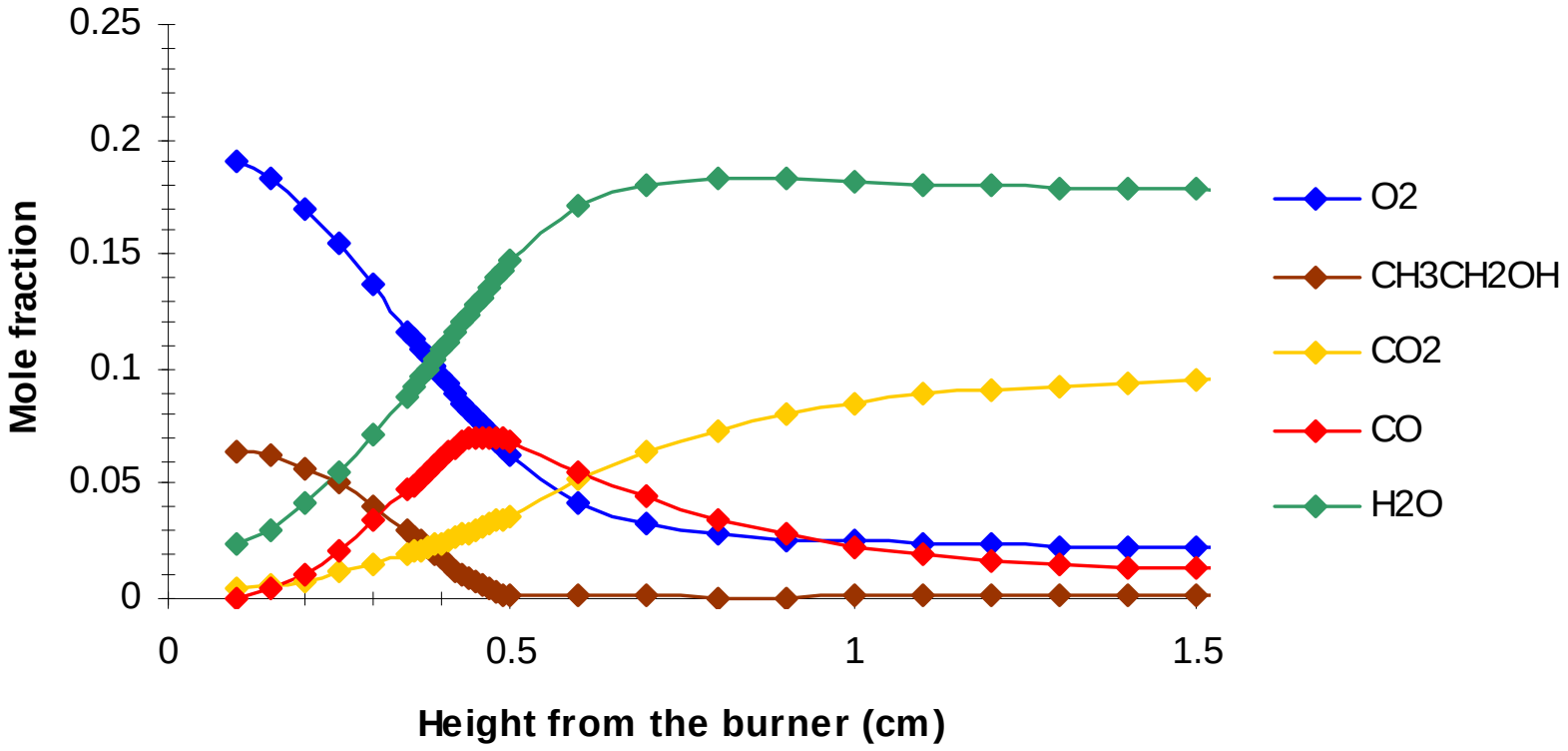

The studied kinetic mechanisms

Name	Number of reactions	Number of species	Efficiency of a third species
Dunphy	97	29	No
M. P. Dunphy, P. M. Patterson et J. M. Simmie, Journal of the Chemical Society Faraday Transactions, volume 87, 1991			
Norton	278	32	Yes
T. S. Norton et F. L. Dryer, International Journal of Chemical Kinetics, Volume 24, 1992			
Dagaut	76	25	No
P. Dagaut, J. C. Boettner et M. Cathonnet, Journal de Chimie Physique et de Physico-Chimie Biologique, volume 89, 1992			
Marinov	383	55	Yes
N. M. Marinov, International Journal of Chemical Kinetics, Volume 31, 1999			

Ethanol

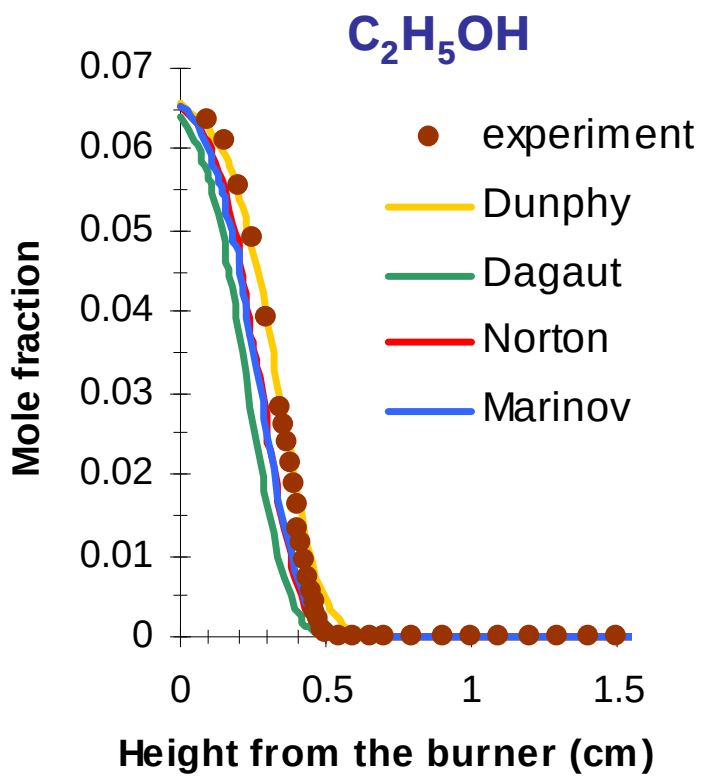

Ethanol consumption main pathways :

- **$CH_3CH_2OH + X = CH_3CHOH + XH$**

Where X is the radical H or OH or O

Norton	**5,2 %**	**44,1 %**	
Marinov	**20,1 %**	**12,3 %**	**5,0 %**

- **$CH_3CH_2OH + X = CH_3CH_2O + XH$**

Where X is the radical H or OH or O

Norton		**17,5 %**	
Marinov	**7,4 %**	**32,3 %**	**1,8 %**

- **$CH_3CH_2OH + X = CH_2CH_2OH + XH$**

Where X is the radical H or OH or O

Norton		**26,5 %**	
Marinov	**11,5 %**	**8,8 %**	**0,8 %**

- **$CH_3CH_2OH = CH_3 + CH_2OH$**

Norton	**6,8 %**

Carbon monoxyde

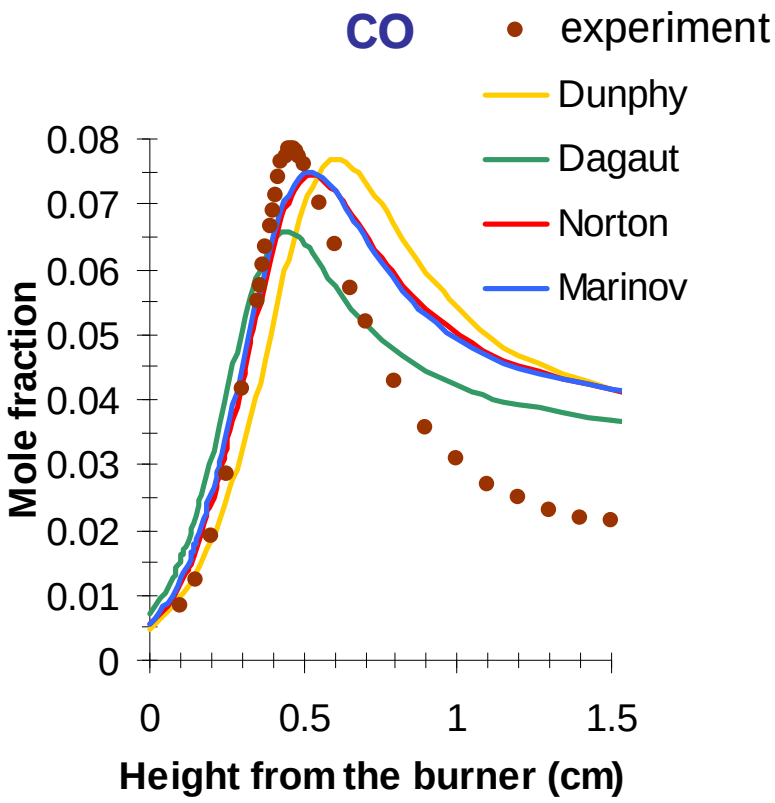

CO Formation main pathways :

- **HCO + X = CO + XH**

Where X is H or OH or O or O_2 or M

Norton 13,2% 22,8% 21,8%

Marinov 16,6% 14,0% 1,8% 36,8% 21,4%

- **$CH_3CO + M = CO + CH_3 + M$**

Norton 42,1%

- **$CH_2 + X = CO + (X - O)H_2$**

Where X is O or O_2

Marinov 6,9% 2,4%

Carbon dioxyde

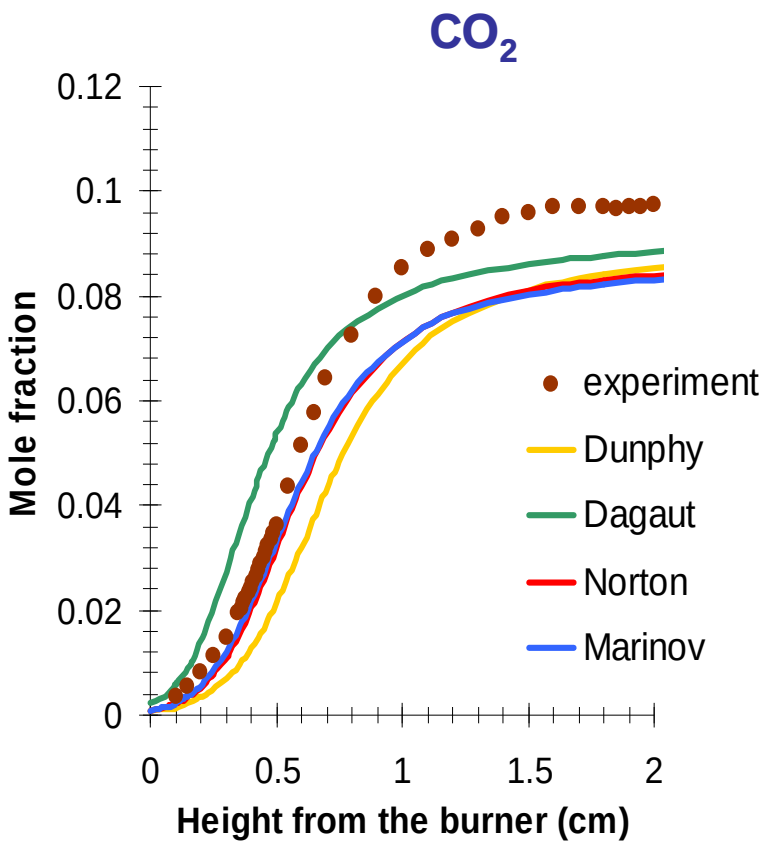

CO_2 Formation main pathway :

- Only one reaction :

$CO + OH = CO_2 + H$ ➡ 100%!

Remark :

- The CO simulated mole fraction profiles are too high
- The CO_2 simulated mole fraction profiles are too low

Conclusion

- We must increase the reaction rate of the precedent reaction

H_2 and O_2

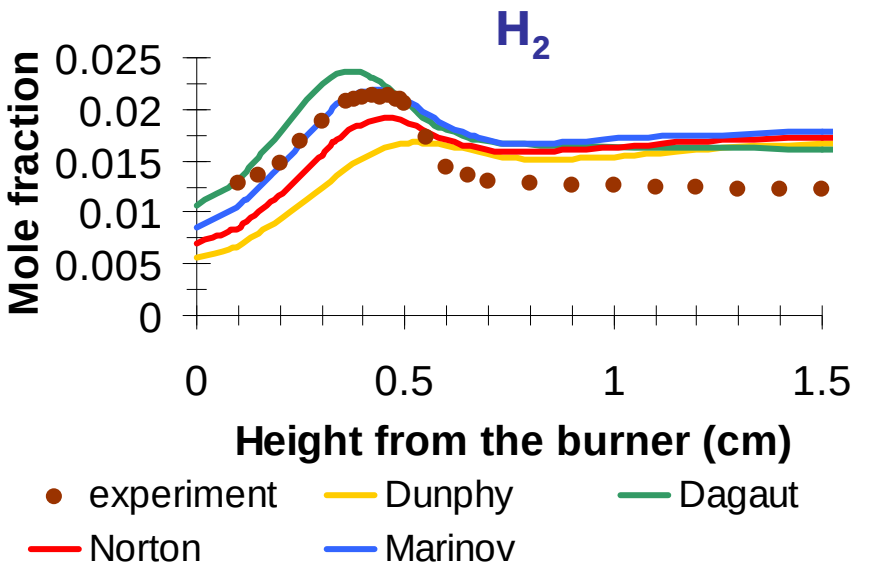

- Good position of the maximum of mole fraction with Norton and Marinov
- Good simulated mole fraction values until 0,5 cm with Marinov
- But overestimation of simulations in the post combustion zone

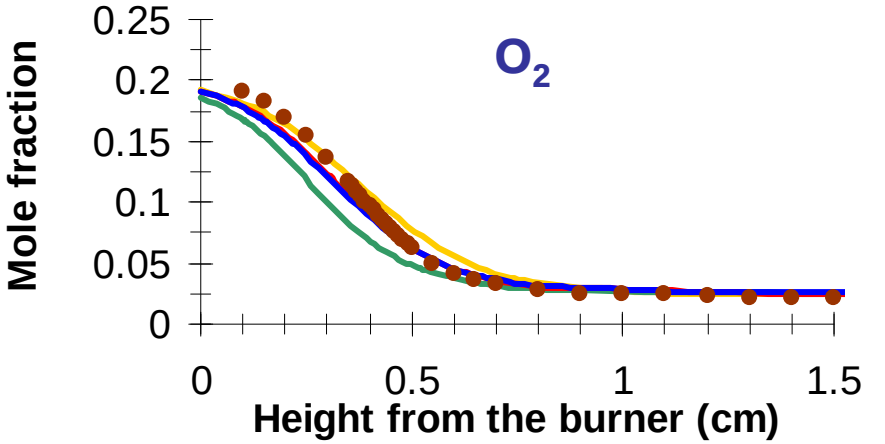

- The experimental profile is very well predicted with the mechanisms of Dunphy, Norton and Marinov
- Modelled consumption is too fast with the mechanism of Dagaut

H_2O and OH

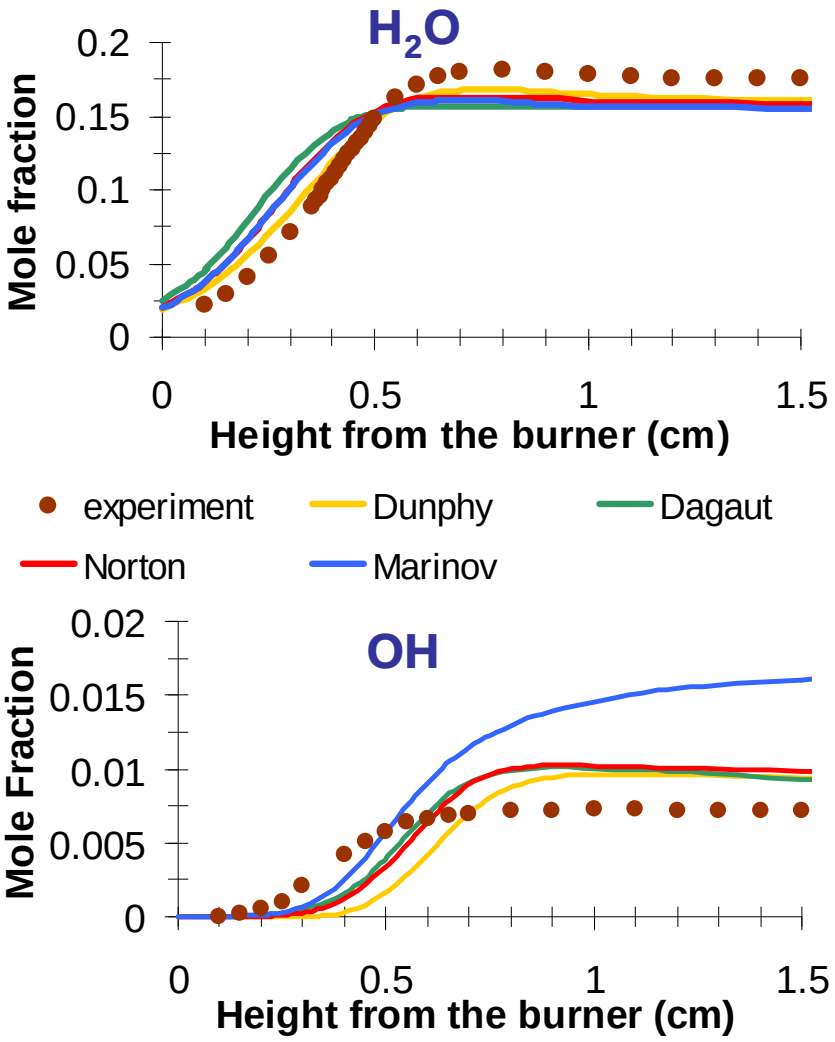

- The experimental profile is well simulated with the mechanism of Dunphy
- Modelled formations are shifted towards the fresh gases region with the mechanism of Dagaut, Norton and Marinov
- The calculated mole fraction values in the burned gases are underestimated
- Simulated formations are too low in the flame front
- In the burned gases, the calculated mole fraction values are too high,
  $\Rightarrow$ especially Marinov

CH_3 and CH_4

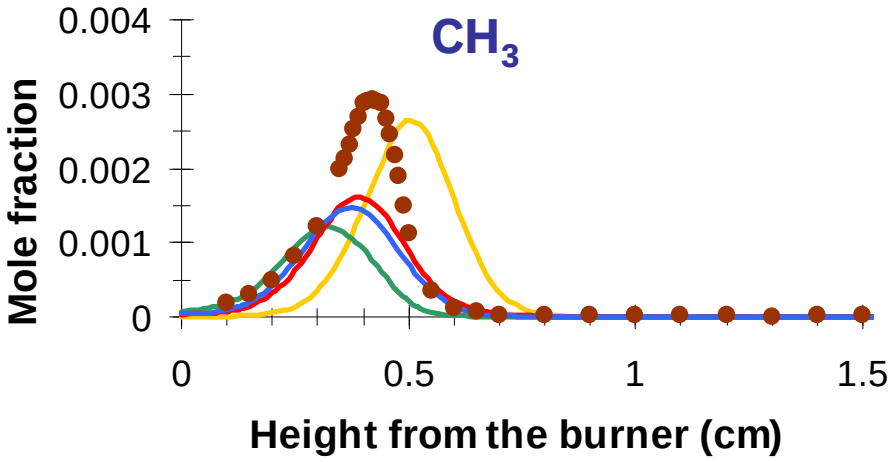

- Position of mole fraction is well simulated with the mechanisms of Norton and Marinov
- The mole fraction values are underestimated by mechanisms

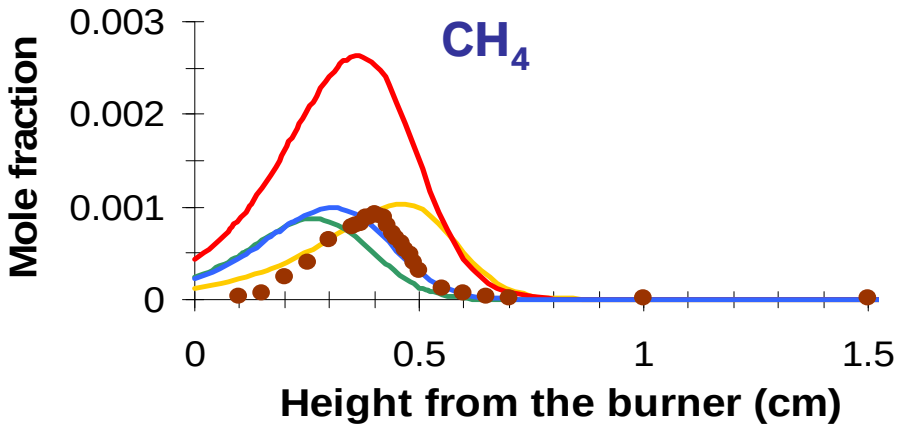

- Maximum mole fractions are well simulated with the mechanisms of Dagaut, Dunphy and Marinov
- The position of the maximum does not match, except with Norton

C_2H_4 and C_2H_2

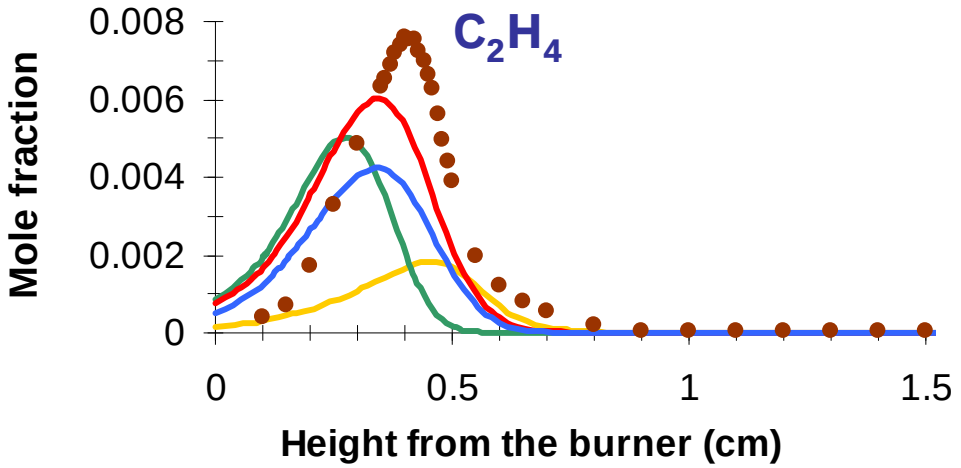

- The position of the calculated maximum is well simulated with the Norton's and the Marinov's mechanisms
- The simulated mole fraction values are underestimated

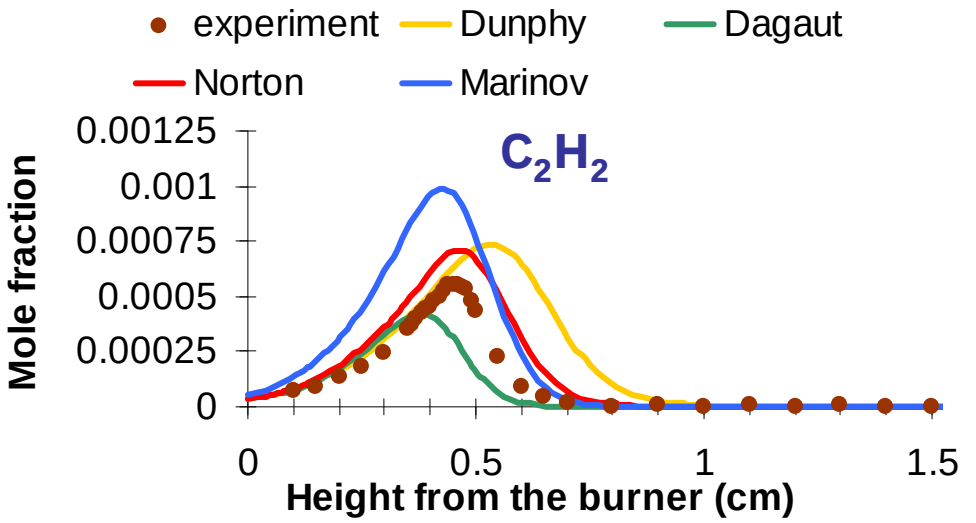

- The experimental profile is very well simulated with the mechanism of Norton
- The acetylene formation is too fast and early with the Marinov model

CH_3HCO and Ar

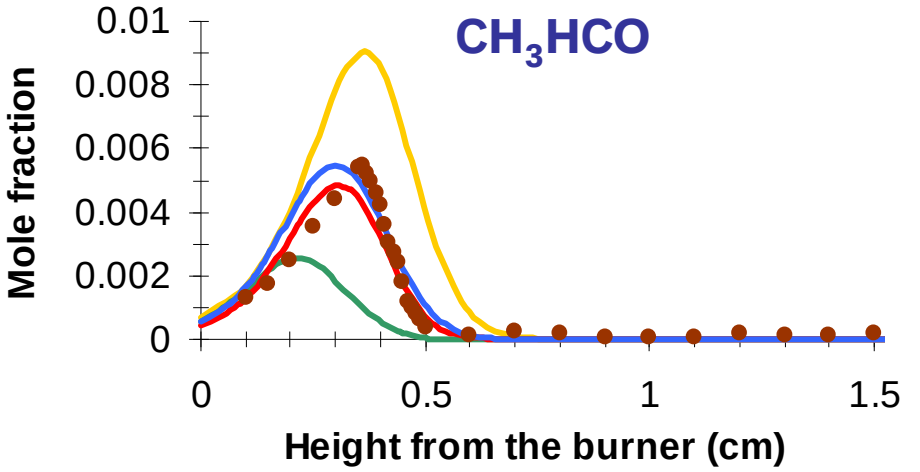

- The experimental profile is very well simulated by the mechanisms of Norton and Marinov
- The position and the maximum mole fraction values disagree with the mechanisms of Dunphy and Dagaut

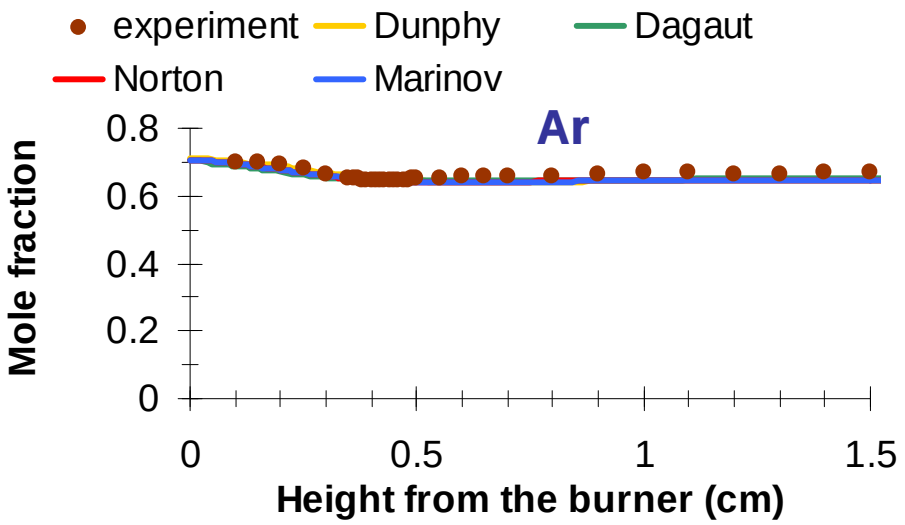

- The experimental profile is well simulated by all mechanisms
- Argon does not allow us to establish the validity of a mechanism in flames

Conclusion about the mechanisms

Mechanism of Dunphy :

- Good agreement for the mole fraction profiles of C_2H_5OH, O_2 and Ar
- The profile positions are generally shifted towards burned gases compared to experimental profiles
- The mole fraction values are not well predicted for H_2, C_2H_2, C_2H_4, CH_3HCO, CO and CO_2

Mechanism of Dagaut :

- Good agreement for the mole fraction profiles of C_2H_5OH, O_2 and Ar
- The profile positions are generally shifted towards fresh gases compared to experimental profiles
- The mole fraction values of intermediate species and products are systematically smaller than the experiment. (except for CH_4)

Cannot be validated by the structure of this ethanol flame (ϕ=1)

Conclusion about the mechanisms

Mechanism of Norton :

- Good agreement for the mole fraction profiles of C_2H_5OH, O_2, Ar, CH_3HCO and C_2H_2
- The positions of the maximum are always well predicted
- The mole fraction values of some profiles are not well predicted : especially for CH_3 and CH_4

Mechanism of Marinov :

- Good agreement for the mole fraction profiles of C_2H_5OH, O_2, Ar and CH_3HCO.
- The profile positions are generally well predicted
- The mole fraction values of some species are not well predicted : OH, C_2H_2, C_2H_4 and CH_3

Best agreement is observed with these mechanisms.
But, the reaction pathways show significant differences between these mechanisms

Common reaction pathways of ethanol consumption

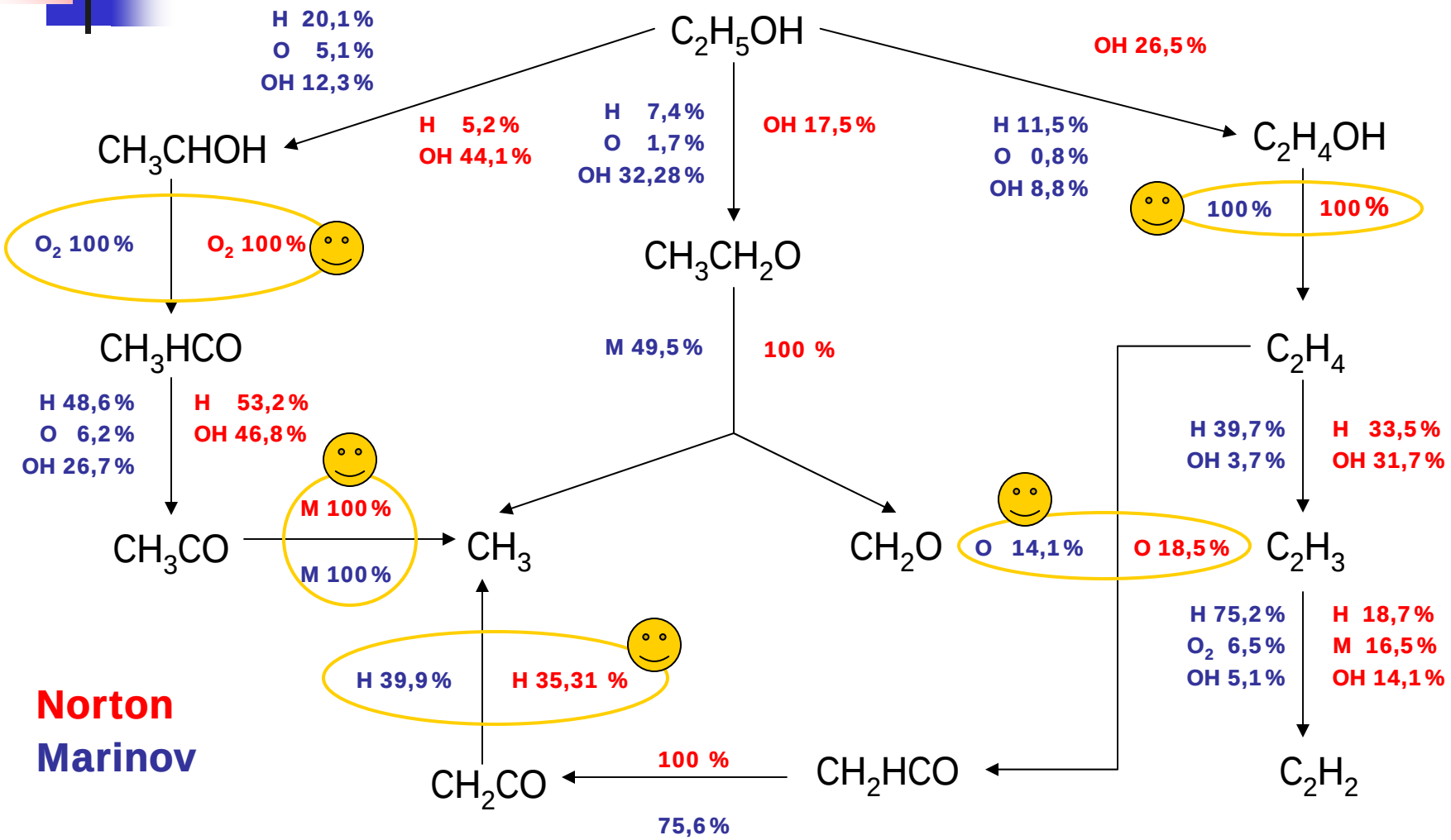

Common reaction pathways of CO_2 formation

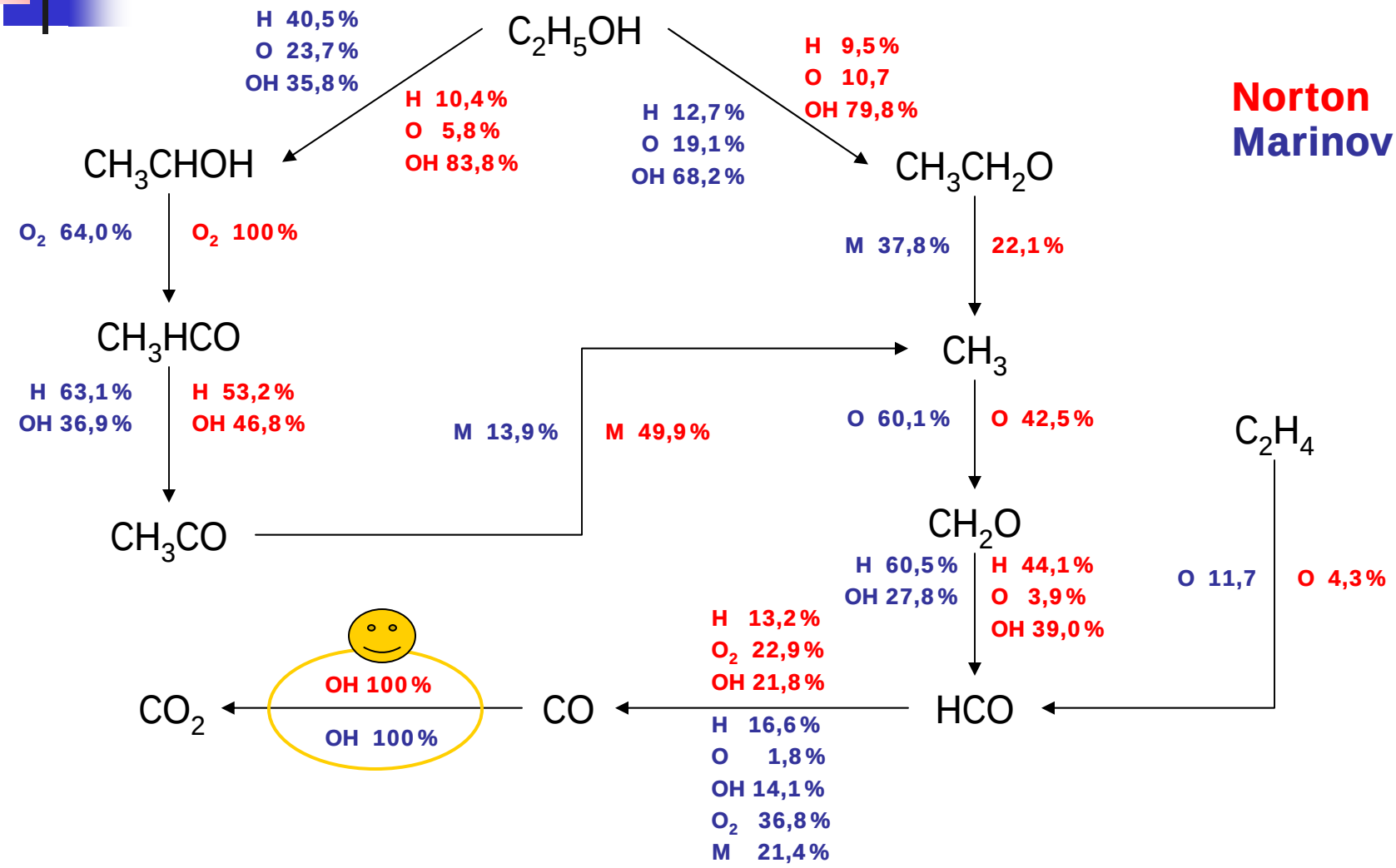

Norton
Marinov

Final conclusion

- A better mechanism should be built
- This new mechanism should be mainly based on the mechanisms of Norton and Marinov
- New experiments must be performed to validate this new mechanism :
  - by measuring mole fraction profiles of other chemical species
  - by checking the validity with various initial conditions like working pressure, equivalence ratio,...

Acknowledgments

Dr. V. Dias

C. Duynslaegher

C. Smets

V. Detilleux

C. Renard

Prof. P.J. Van Tiggelen

Temperature profile : Thermocouple

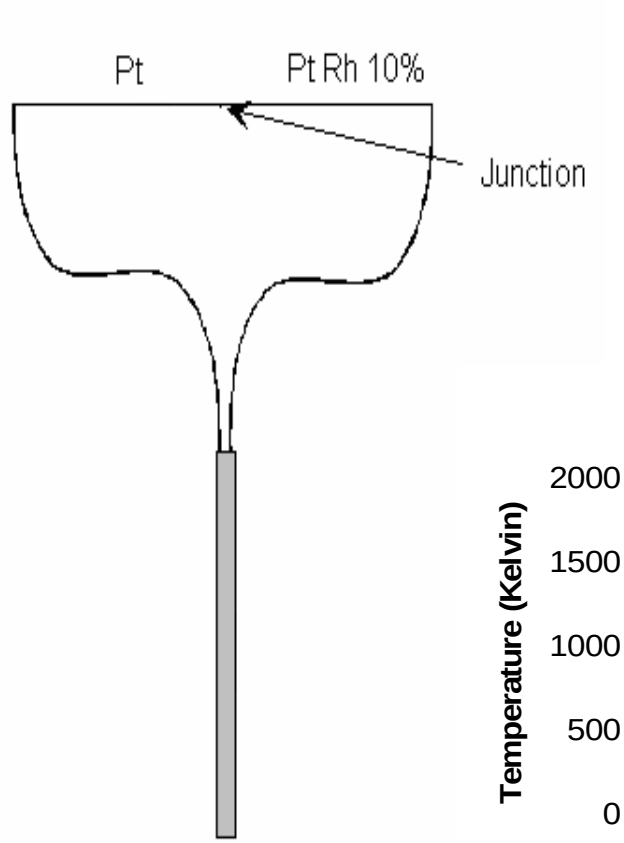

- The potential (mv) at the junction of the two alloys depends on the temperature
- An appropriate function will correlate the voltage with the temperature

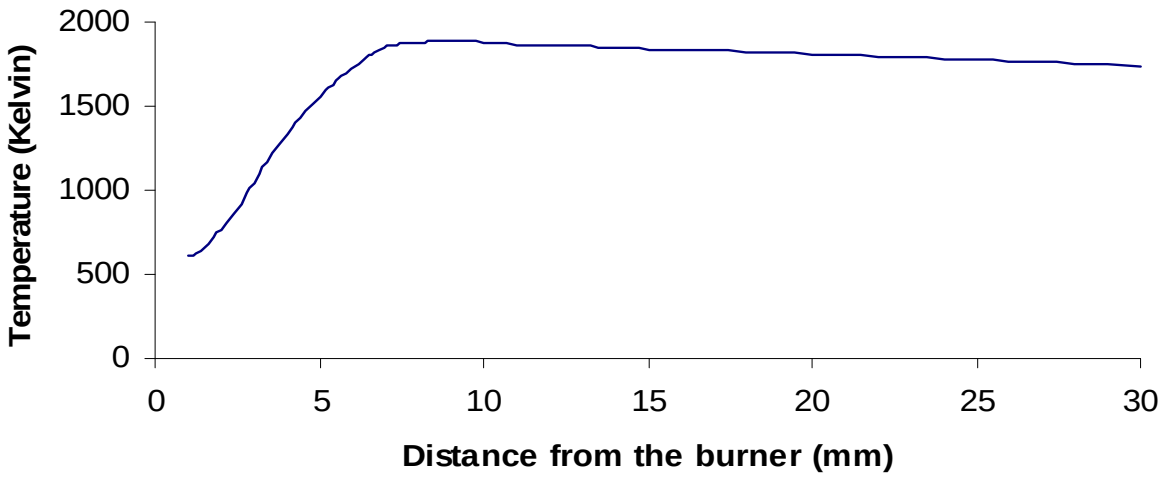

Conversion into mole fraction profiles

- Calibration of each chemical species with an appropriate cool gas mixture wich composition close to these in the flame
  $S_i = X_i / I_i$ -> sensibility factor (s_i)
- Solution of a multiple equation system:

$$\left(X_i\right)_{flame} = \left(\frac{S_j}{S_i}\right)_{mixture} \left(\frac{I_i}{I_j}\right)_{flame} \left(X_j\right)_{flame}$$

j = reference chemical species
i = the other species

$$\sum_i X_i = 1$$

SubTask 2.4F

An experimental study of the structure of a stoichiometric ethanol/oxygen/argon flame

N. Leplat[1], A. Seydi[2], J. Vandooren[1]
[1] CSTR-Laboratoire de Physico-Chimie de la Combustion
Université Catholique de Louvain
Place Louis Pasteur, 1 - 1348 Louvain-La-Neuve - Belgium
[2] Université Cheikh Anta Diop – Dakar – Senegal

Abstract

Experimental mole fractions profiles of stable species and radicals are reported for a stoichiometric ethanol laminar premixed flame $C_2H_5OH/O_2/Ar$ burning at 50 mbar. Different mechanisms are tested by comparison of model predictions with experimental results. The results show that some ethanol mechanisms predict reasonably well reactants and products profiles but significant differences for many intermediate species remain.

Introduction

Nowadays, the future exhaustion of petroleum reserves stimulates the research to find alternative fuels. Among them ethanol is now used as a fuel and it is subjected to many research works. Its production is currently made by fermentation of different biomass products. So ethanol will permit to reduce the dependence with fossil fuels. Furthermore, the combustion of this fuel doesn't increase the total quantity of greenhouse effect gases released in the atmosphere. Therefore, the use of ethanol as a fuel can ensure environmental and energetic benefits even if the impact of the energy input and the use of fertilizers and pesticides are taken into account (Hill et al., 2006 ; von Blottnitz and Curran, 2007 ; Agarwal, 2007).

Ethanol can also be used as an additive for current gasoline. On the one hand, ethanol enables to increase the octane number of a burning mixture and on the other hand it reduces the mass emissions of unburned hydrocarbons and carbon monoxide from current automobiles (Sawyer, 1992) and from combustion devices (Inal and Senkan, 2002 ; Wu et al., 2006 ; Ergut et al., 2006 ; McEnally and Pfefferle, 2007).

For these reasons the understanding of each step of the ethanol combustion and the development of a correct mechanism which can simulate experimental data in an ethanol flame are of the highest importance.

Previous studies have identified the first reaction in the ethanol combustion and the process of solid carbon formation in diffusion flames (Smith and Gordon, 1956), in static reactors (Brown and Tipper, 1969), in shock tubes (Cooke et al., 1971 ; Tsang, 1976) and the use of radioisotopic tracer in diffusion flame (Lieb and Roblee, 1970). These studies have shown that an hydrogen abstraction can occur at three reaction sites, leading to the formation of one of the three isomers of the $C_2H_5O^{\bullet}$ radical. First, due to the weakness of α C-H bonds in the proximity of the electrophilic O atom, the major initial pathway of ethanol consumption gives the radical $CH_3CH^{\bullet}OH$ by the following reaction (Norton and Dryer, 1990 ; Egolfopoulos et al., 1992) :

$CH_3CH_2OH + R^{\bullet} \rightarrow CH_3C^{\bullet}HOH + RH$ (R. 1)

Where $R^{\bullet}$ are $H^{\bullet}$, O or $^{\bullet}OH$. Afterwards molecule of oxygen reacts with the radical to produce acetaldehyde (R. 2) which is able to produce quickly a molecule of carbon monoxide though reaction R. 3 and R. 4 :

$CH_3C^{\bullet}HOH + O_2 \rightarrow CH_3CHO + HO^{\bullet}_2$ (R. 2)

$CH_3CHO + R^{\bullet} \rightarrow CH_3C^{\bullet}O + RH$ (R. 3)

$CH_3C^{\bullet}O \rightarrow {}^{\bullet}CH_3 + CO$ (R. 4)

The second main pathway of reaction is an hydrogen abstraction from the β C-H bonds. Even if these bonds are stronger than the α C-H bonds, they are subjected to radical attack due to the larger number of H atoms linked to the β carbon atom. Furthermore, some studies show that at high temperature the branching ratio of $C_2H_5OH + R^{\bullet}$ shifts to favour the formation of $C^{\bullet}H_2CH_2OH$ radicals (Dutton et al., 1985 ; Grotheer et al., 1986) These radicals loosing an $^{\bullet}OH$ lead to the formation of ethylene (C_2H_4) molecules which can burn according to the classical combustion scheme :

$CH_3CH_2OH + R^{\bullet} \rightarrow C^{\bullet}H_2CH_2OH + RH$ (R. 5)

$C^{\bullet}H_2CH_2OH \rightarrow C_2H_4 + {}^{\bullet}OH$ (R. 6)

Thirdly, although O-H bond energies (D(O-H) = 436 kJ/mol) are greater than the C-H bond energies ($D(C_{\alpha}\text{-}H)$ = 397 kJ/mol and $D(C_{\beta}\text{-}H)$ = 424 kJ/mol), H atom abstraction from the OH groups occurs during the alcohol combustion (Hess and Tully, 1989). The ethoxy radical is decomposed principally by β-scission of one C-H bonds (R. 8) or by β-scission of the C-C bond (R. 9) :

$CH_3CH_2OH + R^{\bullet} \rightarrow CH_3CH_2O^{\bullet} + RH$ (R. 7)

$CH_3CH_2O^{\bullet} \rightarrow CH_3CHO + H^{\bullet}$ (R. 8)

$CH_3CH_2O^{\bullet} \rightarrow {}^{\bullet}CH_3 + CH_2O$ (R. 9)

Finally, the last reaction of the initial degradation of ethanol is the direct dissociation of the fuel by the scission of the C-C bond (R. 10) (Barnard and Hughes, 1960). The radical $C^{\bullet}H_2OH$ reacts with oxygen (R. 11) or decomposes to give formaldehyde (R. 12) :

$CH_3CH_2OH \rightarrow {}^{\bullet}CH_3 + C^{\bullet}H_2OH$ (R. 10)

$C^{\bullet}H_2OH + O_2 \rightarrow CH_2O + HO^{\bullet}_2$ (R. 11)

$C^{\bullet}H_2OH + M \rightarrow CH_2O + H^{\bullet} + M$ (R. 12)

Note that the combustion of ethanol leads quickly to oxygenated molecules (acetaldehyde and formaldehyde). At the opposite, the formation of oxygenated intermediates in the alkane combustion occurs by the reaction of an alkene intermediate with O atoms, O_2 or $HO^{\bullet}_2$.

The next step of the understanding of the ethanol combustion was the development of an accurate kinetic mechanism which includes the ensemble of rate constants associated to each reaction.

In 1981, Natarajan and Bhaskaran (1981) have proposed an ethanol oxidation mechanism using experimental data together with estimated rate coefficients for unknown processes.

Later, Dunphy et al. (1991b) published a 97-step for a 30 species reaction mechanism. This mechanism is based on a methanol oxidation model completed with additional reactions involving ethanol, acetaldehyde and $CH_3C^{\bullet}HOH$, $CH_3CH_2O^{\bullet}$ and $CH_3C^{\bullet}O$ radicals. This mechanism was validated against ignition delays in shock tubes measurements (Dunphy et al., 1991a ; Curran et al., 1992) and some kinetic constants were optimized by a sensitivity analysis.

Afterwards, Norton and Dryer (1992) have built a 142-step detailed oxidation mechanism based on a review of the literature for rate coefficients of elementary reactions occurring in the ethanol oxidation. The authors emphasize the importance of the three distinct H-atoms sites and so include the three isomeric forms of $C_2H_5O^{\bullet}$. This mechanism shows good agreement in comparison with ethanol oxidation experiments performed in turbulent flow reactors at 1100 K and at atmospheric pressure (Norton and Dryer, 1990) .

At the same time, Dagaut et al. (1992) published an ethanol sub-mechanism composed of 39 reactions. Kinetic parameters for ethanol consumption were selected from different previous studies (Tsang, 1976 ; Pitz et al., 1988 ; Grotheer et al., 1986 ; Walker, 1975, 1976 ; Kerr and Parsonage, 1976). This mechanism was evaluated by comparison with experimental data coming from ethanol pyrolysis in a flow reactor (Rotzoll, 1985), from ethanol oxidation in a jet-stirred reactor (Dagaut et al., 1992), from ethanol-air flame burning velocities (Gülder, 1982) and from ethanol-O_2-Ar ignition delays measured in shock tubes (Natarajan and Bhaskaran, 1981 ; Dunphy et al., 1991a, 1991b).

Marinov (1999) has developed a detailed chemical kinetic model representing the high temperature ethanol oxidation. He calculates branching ratios as function of temperature for each H-abstraction reaction with $^{\bullet}OH$, O, $^{\bullet}CH_3$, $H^{\bullet}$ and $HO^{\bullet}_2$ radicals, and the rate constants associated by analogy with compounds that exhibit similar structural and chemical bonding characteristics (propane and methanol). Moreover, rate coefficients for decomposition reactions were calculated by RRKM/Master equation calculations. The Marinov's mechanism has been validated against à variety of experimental data including laminar flame burning velocities (Gülder, 1982 ; Egolfopoulos et al., 1992), ignition delays measured in reflected shock waves (Natarajan and Bhaskaran, 1981 ; Dunphy et al., 1991a, 1991b) and ethanol oxidation products profiles in jet-stirred (Dagaut et al., 1992) and turbulent flow reactors (Norton and Dryer, 1992).

More recently, new efforts are made to improve the knowledge of the rate coefficients of the ethanol combustion reactions. Li et al. (2004, 2005) have calculated from pyrolysis data new rate constants for ethanol decomposition reactions and have developed a new ethanol oxidation mechanism based on experiments performed in a variable pressure flow reactor.

Unfortunately, there are few ethanol flame structure data available (Tanoff et al., 1992) for comparison with these modelling works. In order to fill the gap, we measured for a maximum of stable species and radicals, their mole fraction profiles in a stoichiometric flame stabilised at low pressure. The comparison of our experimental measurements with simulated data shows that

intermediate species profiles are generally not well predicted by the above mentioned mechanisms.

Experimental

The experimental setup used to determine the structure of one-dimensional laminar premixed flames has been described previously (Vandooren et al., 1992) and it is illustrated schematically in figure 1. Briefly, it consists of a molecular beam mass spectrometer system (MBMS) coupled to a combustion chamber and a quartz nozzle which enable us to sample in the flame. The flat flame burner consists of a cooled, brass, sintered plate housed in a vacuum chamber maintained at 50 mbar. The sampling position in the flame is varied by moving the burner in order to modify the distance with the quartz cone. The molecular beam emanating from the sampling cone is accelerated through differentially pumped chambers towards the ion source of the mass spectrometer where it is ionised by an electron beam.

The electron beam energies are selected for each species analysed in order to obtain a signal-to-noise ratio high enough without interference from an eventual fragmentation of other species.

The deduction of mole fraction profiles from intensity profiles has been achieved by means of the sensitivity factors (S_i) which links the signal intensity (I_i) with the mole fraction (X_i), for each species at a given temperature :

$$I_i = S_i X_i$$

Mahnen (1973) has shown that the sensitivity factor varies in the same manner as a function of temperature for all species. Therefore, the ratio of sensitivity factors of two species (S_i/S_j) remains constant at every distance in the flame. So, we can deduce mole fraction profiles for each species by solving the following equations system :

$$\frac{S_i}{S_j} = \frac{I_i X_j}{I_j X_i}$$

$$\sum X_i = 1$$

Ratios of sensitivity factors are measured at room temperature with appropriate cold gas mixtures. For labile species (Z), sensitivity factors have been estimated by a comparative calibration with the nearest stable species (Y) by using the additivity of the individual element contribution through the equation :

$$\frac{S_Z}{S_Y} = \frac{(1.8n_C + 0.65n_H + 1.3n_O)_Z}{(1.8n_C + 0.65n_H + 1.3n_O)_Y}$$

where n_i is the number of atoms i in the molecule.

High purity ethanol (99.99%), oxygen (99.5%) and argon (99.99%) were used for preparing the initial gas mixture. Initial operating conditions of the flame used in the current study are presented in Table 1.

Finally, the temperature (figure 2) profile has been measured by using a 0.1mm diameter Pt/PtRh 10% thermocouple coated with Y_2O_3-BeO ceramic in order to prevent catalytic reactions on the platinum wire (Kent, 1970). Radiation losses have been corrected by electrical compensation. The measured maximum temperature is 1884 K.

Modeling of the stoichiometric ethanol flame

Simulations were performed to check the validity against experimental mole fraction profiles of four detailed kinetic mechanisms previously published in the literature. These models were assembled by Dunphy et al. (1991), Norton and Dryer (1992), Dagaut et al. (1992), and Marinov (1999). The Dagaut et al. mechanism concerning the direct oxidation of ethanol has been completed by some kinetic parameters coming from the Marinov (1999) and the Dias et al. (2003) mechanisms respectively for reactions involving methanol and lower species. The characteristics of each mechanism are summarized at the table 2.

Modelling computations were performed by using the PREMIX code (Kee et al., 1993). Transport properties and thermochemical quantities from the Burcat's (2007) database were used. The same set of properties were used for all the models. Furthermore the experimental temperature profile has been introduced as an input parameter.

Simulated and experimental mole fraction profiles for reactants and products are shown in figure 3. In general, simulations agree reasonably well for these species but the degree of accord will depend on the model used and this means that some improvements must be made.

We observe also those profiles are identically predicted by Norton and Marinov mechanisms although the prediction of Dagaut is shifted strongly upwards while that of Dunphy shifts downwards. This fact is also observed for intermediate specie profiles.

Reaction rate flow calculations have been performed for Norton and Marinov Mechanisms. Figures 4 and 5 present the main consumption pathways of ethanol issuing from both mechanisms. Because the list of elementary reactions are very similar between Norton and Marinov models, main differences between both mechanisms arise from the kinetic parameters selected. The rate analysis has allowed us to identify the origin of discrepancies between simulated mole fractions profiles. Indeed, we notice that the impact of reaction pathways is significantly different between these mechanisms. In fact only the five following reactions have the same importance in the two schemata of ethanol consumption despite the fact that the assigned rate constants are different for both authors :

$CH_3C^{\bullet}HOH + O_2 \rightarrow CH_3CHO + HO^{\bullet}_2$ (R. 2)

$CH_3C^{\bullet}O + M \rightarrow {}^{\bullet}CH_3 + CO + M$ (R. 4)

$C^{\bullet}H_2CH_2OH \rightarrow C_2H_4 + {}^{\bullet}OH$ (R. 6)

$CH_2CH_2 + O \rightarrow C^{\bullet}H_2CHO + H^{\bullet}$ (R. 13)

$CH_2CO + H^{\bullet} \rightarrow {}^{\bullet}CH_3 + CO$ (R. 14)

Therefore, even if ethanol consumption rate are quite similar by using Norton or Marinov mechanisms, branching ratios of each type of ethanol degradation remain different as it is

summarized in table 3. This fact leads to discrepancies observed for the mole fraction profiles of intermediate species.

Mole fraction profiles of main intermediate species have been measured and are presented in figure 6. We observe more divergences between models and experimental data than for the main species profiles. These comparisons for intermediate species show that any mechanism is presently able to simulate correctly the ethanol flame structure. However, the best agreement is observed for the Norton and the Marinov mechanisms which predict correctly the position of the maximum of each mole fraction profile.

In the case of CH_3CHO, the Norton mechanism ascribes its formation solely to the radical $CH_3C^{\bullet}HOH$ (R. 2) whereas the Marinov mechanism additionally includes a channel from the radical $CH_3CH_2O^{\bullet}$ (R. 8). Hence, the Marinov model gives a better account of the quantities of CH_3CHO formed in the flame (figure 6), because more of the ethanol consumption is being routed through the aldehyde channel (Table 3).

C_2H_4 molecules are only formed according both authors from the radical $C^{\bullet}H_2CH_2OH$ (R. 6). Table 3 shows that the percentage of formation of this species is almost similar for Norton and Marinov. Nevertheless the modelled profiles for this species are underestimated by all mechanisms. The reason can be a wrong estimate of the branching ratio of the three hydrogen abstraction reactions (R. 1, R. 5 and R. 7) or an overestimate of the reaction rate and of the kinetic parameters of the C_2H_4 consumption reactions.

The C_2H_2 molecule is according to Norton and Marinov only formed by two successive hydrogen atom abstractions from C_2H_4 by $H^{\bullet}$ and $^{\bullet}OH$ radicals. Table 4 indicates that the percentage of ethanol which leads to the formation of C_2H_2 is similar for Marinov and for Norton mechanisms. The overestimate of C_2H_2 profile by Norton and especially by Marinov signifies that the reaction rate of C_2H_2 is probably too slow. An overestimate of the reaction rates for the combustion of C_2H_4 leading to C_2H_2, can also be the source of the high mole fraction value predicted. Note that, a better evaluation of the reaction rate of these reactions can improve both C_2H_2 and C_2H_4 predictions. However, the kinetic parameters proposed by Norton for reactions concerning the conversion of C_2H_4 into C_2H_2 and the oxidation of C_2H_2 lead to a better agreement with experimental results.

The formation of $^{\bullet}CH_3$ occurs along several reaction pathways including the degradation of CH_3CHO and C_2H_4 and the breaking of the C-C bond in the CH_3CH_2OH (R. 10) molecule or in the $CH_3CH_2O^{\bullet}$ radical (R. 9). Once again, table 4 shows that the percentage flux from ethanol to methyl radical is different for both mechanisms. Furthermore, Dagaut, Norton and Marinov simulations underestimate the experimental profile of the $^{\bullet}CH_3$ radical. This fact is not due to a wrong estimate of the first degradation steps of ethanol knowing that a large part of the combustion pathways involves this intermediate species. So, the solution is a better assessment of the $^{\bullet}CH_3$ consumption kinetic parameters.

The molecule of CH_4 is an intermediate of lesser importance in ethanol flames. Its accumulation in the reaction zone is more due to its relative weak reactivity rather than a high rate of formation. CH_4 is formed from the radical $^{\bullet}CH_3$ and it is consumed to give this same radical. The profiles of these species show that the kinetic parameters of Dunphy seem to represent perfectly the reaction between $^{\bullet}CH_3$ and CH_4 occurring in the flame.

Finally our experimental work have ensured to measure a mole fraction profile for the •OH radical. This species is one of the most reactive in all combustion systems. Then, a wrong simulation of the •OH radical profile can induce a general problem. It is possible that part of the discrepancy obtained with the Marinov simulation is due to a bad estimation of this radical profile especially in the burned gases.

Conclusion

The comparison between simulated and experimental profiles have shown that any mechanism is actually able to be validated for a stoichiometric ethanol flame. Indeed we observe only a good agreement for main species profiles. None of these mechanisms do a good job of fitting the minor species. These models are now quite dated and almost certainly need re-vamping in light of more recent works. The rate contribution analysis has shown that the problem can probably be solved by a better evaluation of some kinetic parameters. So this work can be the basis of the building of a new ethanol mechanism or an improvement of the Norton or Marinov mechanisms.

Acknowledgments

Authors are grateful to the Région Wallonne for the financial support (visa 06/47214)

References

Agarwal, A.K. (2007) Biofuels (alcohols and biodiesel) applications as fuels for internal combustion engines. *Prog. Energy Comb. Sci.*, 33, 233-271.

Barnard, J.A. and Hughes, H.W.D. (1960) The Pyrolysis of Ethanol. *Trans. Faraday Soc.*, 56, 55-63.

Brown, J. and Tipper, C.F.H. (1969) The Cool Flame Combustion of Ethanol. *Proc. Royal Soc.*, A312, 399-415.

Burcat, A. (2007) Ideal Gas Thermodynamic Data in Polynomial form for Combustion and Air Pollution Use. *http://garfield.chem.elte.hu/Burcat/burcat.html*.

Cooke, D.F., Dodson, M.G. and Williams, A. (1971) A Shock-Tube Study of the Ignition of Methanol and Ethanol with Oxygen. *Combust. Flame*, 16, 233-236.

Curran, H.J., Dunphy, M.P., Simmie, J.M., Westbrook, C.K. and Pitz, W.J. (1992) Shock Tube Ignition of Ethanol, Isobutene and MTBE: Experiment and Modeling, *Proc. Combust. Instit.*, 24, 769-776.

Dagaut, P., Boettner, J.C. and Cathonnet, M. (1992) Kinetic Modeling of Ethanol Pyrolysis. *J. Chim. Phys.*, 89, 867-884.

Dias, V. (2003) *PhD Thesis Université Catholique de Louvain*, Belgium.

Dias, V., Renard, C., Van Tiggelen, P.J. and Vandooren, J. (2003) *Proc. of European Combustion Meeting,* 221.

Dunphy, M.P. and Simmie, J.M. (1991a) High-temperature Oxidation of Ethanol Part 1. Ignition Delays in Shock Waves. *J. Chem. Soc. Faraday Trans.*, 87 (11), 1691-1696.

Dunphy, M.P., Patterson, M.P. and Simmie, J.M. (1991b) High-temperature Oxidation of Ethanol Part 2. Kinetic Modelling. *J. Chem. Soc. Faraday Trans.*, 87 (16), 2549-2559.

Dutton, N.J., Fletcher, I.W. and Whitehead, J.C. (1985) Dynamics of Hydrogen Atom Abstraction in the Reaction $O(^3P)$ + Ethanol. *J. Phys. Chem.*, 89, 569-570.

Egolfopoulos, F.N., Du, D.X. and Law, C.L. (1992) A Study on Ethanol Oxidation Kinetics in Laminar Premixed Flames, Flow Reactors and Shock Tubes, *Proc. Combust. Instit.*, 24, 833-841.

Ergut, A., Granata,, S., Jordan, J., Carlson J., Howard, J.B., Richter, H. and Levendis, Y.A. (2006) PAH Formation in One-Dimensional Premixed Fuel-Rich Atmospheric Pressure Ethylbenzene and Ethyl Alcohol Flames. *Combust. Flame* 144, 757-772.

Grotheer, H.H., Nesbitt, F.L. and Klemm, R.B. (1986) Absolute Rate Constant for the Reaction of $O(^3P)$ with Ethanol. *J. Phys. Chem.*, 90, 2512-2518.

Gülder, O.L. (1982) Laminar Burning Velocities of Methanol, Ethanol and Isooctane-Air Mixture. *Proc. Combust. Instit.*, 19, 275-281.

Hess, W.P. and Tully, F.P. (1989) Hydrogen-Atom Abstraction from Methanol by OH. *J. Phys. Chem.*, 93, 1944-1947.

Hill, J., Nelson, E., Tilman, D., Polasky, S. and Tiffany, D. (2006) Environmental, economic, and energetic costs and benefits of biodiesel and ethanol biofuels. *Proc. Nat. Acad. Sci. USA*, 103 (30), 11206-11210.

Inal, F. and Senkan, S.M. (2002) Effects of Oxygenate Additives on Polycyclic Aromatic Hydrocarbons. *Combust. Sci. and Tech.*, 174 (9), 1-19.

Kee, R., Rupley, F.M. and Miller, J.A. (1993*) Sandia Report*, SAND89-8009B.UC-706.

Kent, J.H. (1970) A Noncatalytic Coating for Platinum-Rhodium Thermocouples. *Combust. and Flame*, 14, 279-282.

Kerr, J.A. and Parsonage, M.J. (1976) Evaluated Kinetic Data on the Gas Phase Hydrogen Transfer Reactions of Methyl Radicals. Butterworths, London, 98.

Li, J., Kazakov, A. and Dryer, F.L. (2004) Experimental and Numerical Studies of Ethanol Decomposition Reaction. *J. Phys. Chem. A*, 108, 7671-7680.

Li, J., Kazakov, A. and Dryer, F.L. (2005) Chemical Kinetics of Ethanol Oxidation, *Proc. of the European Combustion Meeting*, 2.

Lieb, D.F. and Roblee Jr., L.H.S. (1970) A Radioisotopic Tracer Study of Carbon Formation in Ethanol-Air Diffusion Flames *Combust. Flame*, 14, 285-296.

Mahnen, G. (1973) *Ph D. Thesis Université Catholique de Louvain*, Belgium.

Marinov, N.M. (1999) A Detailed Chemical Kinetic Model for High Temperature Ethanol Oxidation. *Int. J. Chem. Kinet.,* 31, 183-220.

McEnally, C.S. and Pfefferle, L.D. (2007) The Effects of Dimethyl Ether and Ethanol on Benzene and Soot Formation in Ethylene Nonpremixed Flames, *Proc. Combust. Instit.*, 31, 603-610.

Natarajan, K. and Bhaskaran, K.A. (1981) *International Symp. On Shock Tubes and Waves*, 13, 834-842.

Norton, T.S. and Dryer, F.L. (1990) The Flow Reactor oxidation of C_1-C_4 Alcohols and MTBE, *Proc. Combust. Instit.,* 23, 179-185.

Norton, T.S. and Dryer, F.L. (1992) An Experimental and Modeling Study of Ethanol Oxidation Kinetics in an Atmospheric Pressure Flow Reactor, *Int. J. Chem. Kinet*., 24, 319-344.

Pitz, W.J., Wilk, R.D., Westbrook, C.K. and Cernansky, N.P. (1988) The oxidation of N-butane at low and intermediate temperatures: An experimental and modeling study, *Western States Section, The Combustion Institute, spring meeting*, 38.

Rotzoll, G. (1985) High-temperature pyrolysis of ethanol. *J. Anal. Appl. Pyrol.*, 9 (1), 43-52.

Sawyer, R.F. (1992) Reformulated Gasoline for Automotive Emissions Reduction, *Proc. Combust. Instit*., 24, 1423-1432.

Smith, S.R. and Gordon, A.S. (1956) Studies of Diffusion Flames. II. Diffusion Flames of Some Simple Alcohols. *J. Phys. Chem.*, 60, 1059-1062.

Tanoff, M.A., Schear, D.M., Olsson, J.O. and Andersson, L.A. (1992) Combustion of Ethanol in Laminar Flames : Probing with Continuous Microprobe Sampling Mass Spectrometry. *Bull. Soc. Chim. Belg.*, 101, 839-850.

Tsang, W. (1976) Thermal Stability of Alcohols. *Int. J. Chem. Kinet.*, 8, 173-192.

Vandooren, J., Branch, M.C. and Van Tiggelen, P.J. (1992) Comparisons of the Structure of Stoichiometric CH_4-N_2O-Ar and CH_4-O_2-Ar Flames by Molecular Beam Sampling and Mass Spectrometric Analysis. *Combust. and Flame*, 90, 247-258.

von Blottnitz, H. and Curran, M.A. (2007) A review of assessments conducted on bio-ethanol as a transportation fuel from a net energy, greenhouse gas, and environmental life cycle perspective. *J. of Clean. Prod.*, 15, 607-619.

Walker, R.W. (1975) A Specialist Periodical Report, Reaction Kinetics, Vol. 1, *The Chemical Society, London* ; (1977) Gas Kinetics and Energy Transfer, Vol. 2, *The Chemical Society, London*.

Wu, J., Song, K.H., Litzinger, T., Lee, S.Y., Santoro, R., Linevsky, M., Colket, M. and Liscinsky, D. (2006) Reduction of PAH and Soot in Premixed Ethylene-Air Flames by Addition of Ethanol. *Combust. Flame* 144 675-687.

Figures and tables

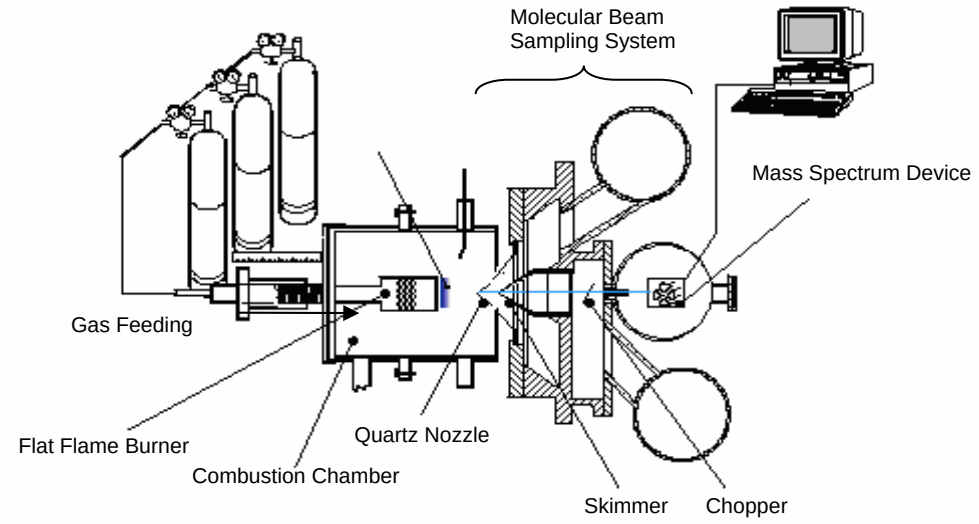

Figure 1 : Schematic diagram of the molecular beam mass spectrometer sampling system (MBMS)

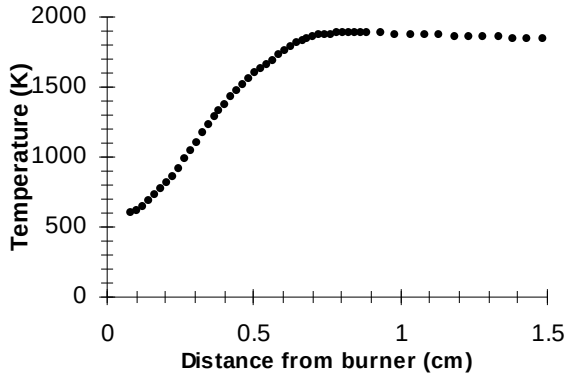

Figure 2 : Experimental temperature profile measured by using a Pt/PtRh 10% thermocouple

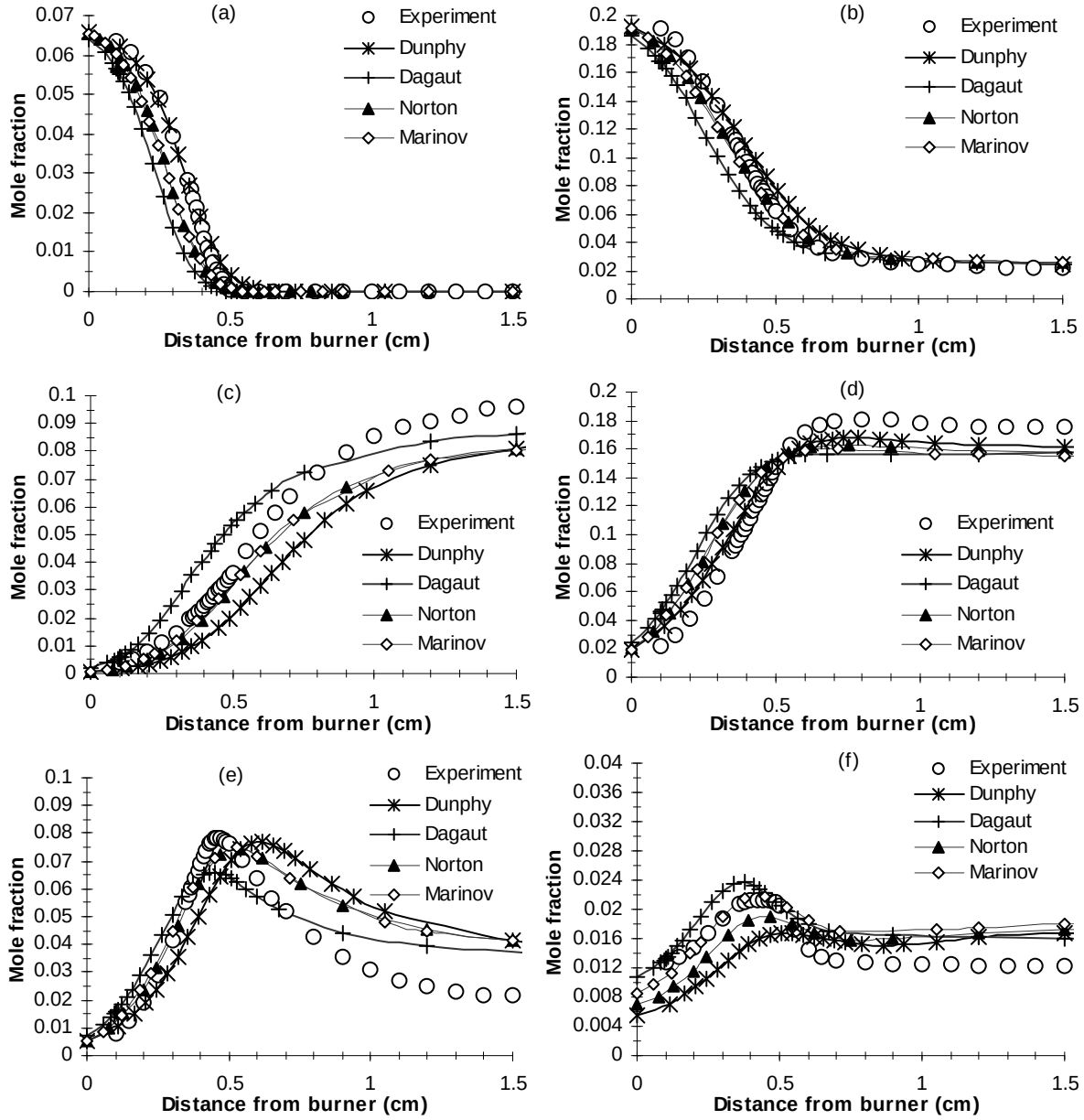

Figure 3 : Experimental and computed mole fraction profiles of reactants and products in a stoichiometric ethanol/oxygen/argon flame : (a) C_2H_5OH, (b) O_2, (c) CO_2, (d) H_2O, (e) CO and (f) H_2.

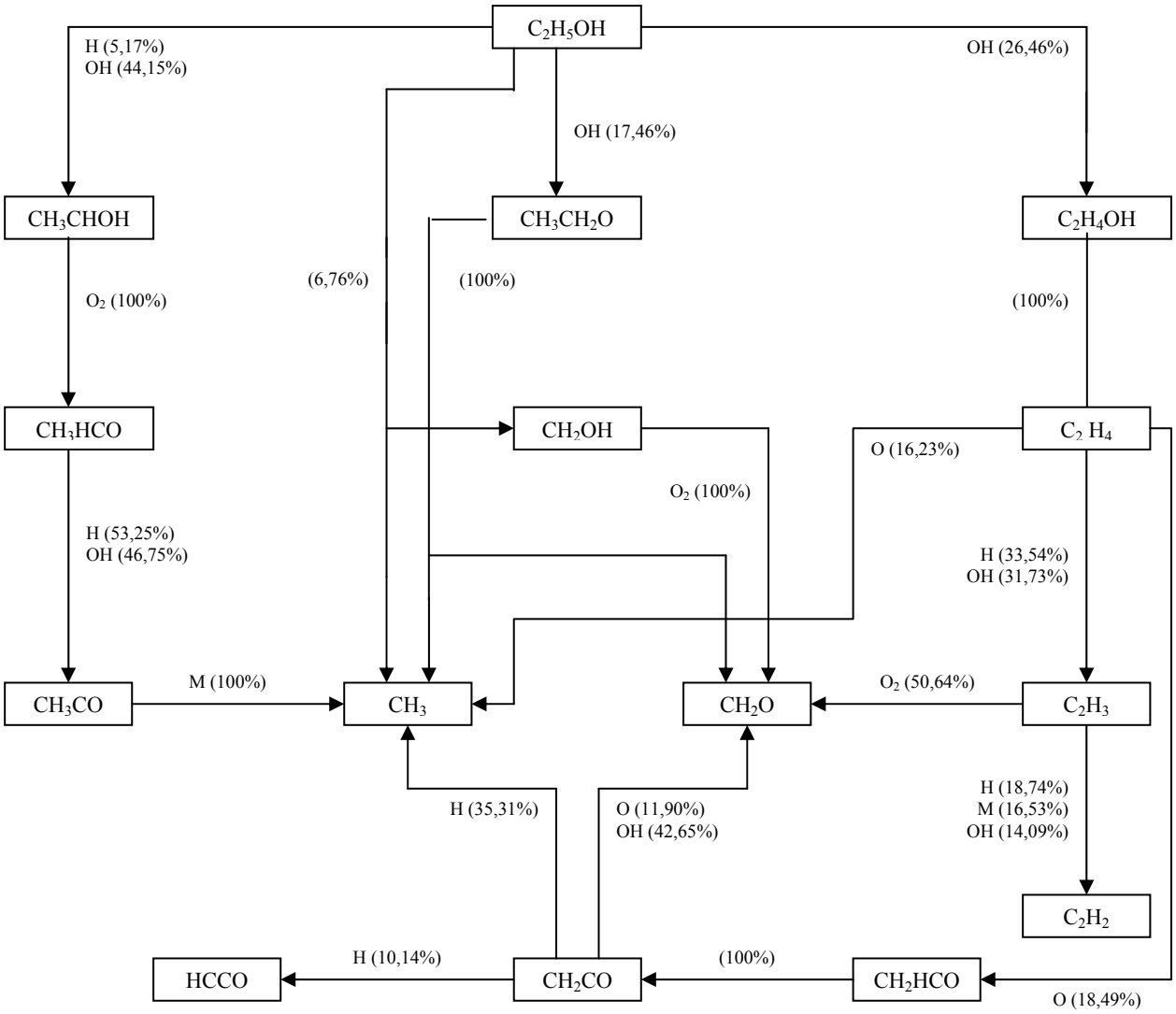

Figure 4 : Main consumption pathways issuing from Norton's mechanism

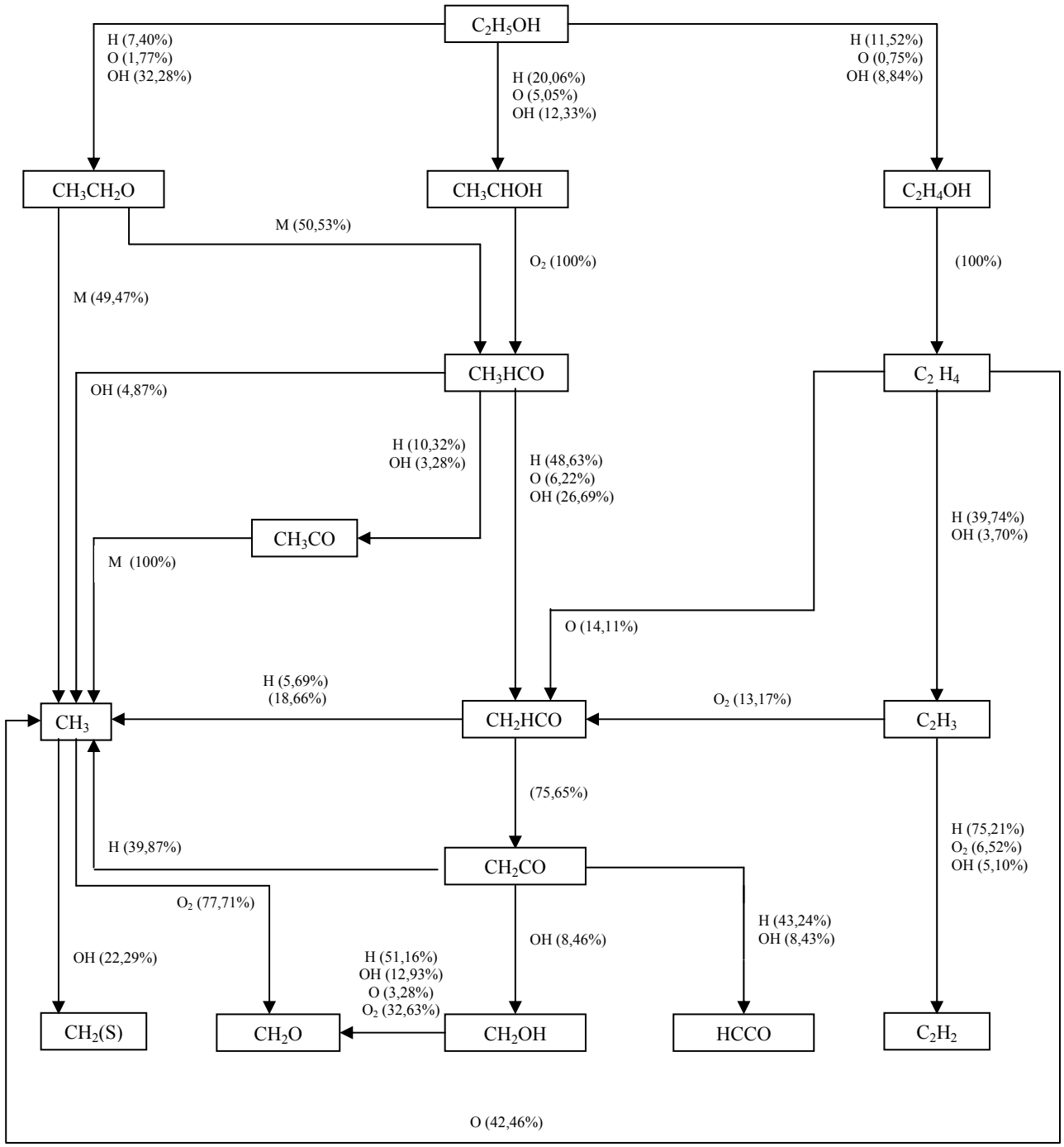

Figure 5 : Main consumption pathways issuing from Marinov's mechanism

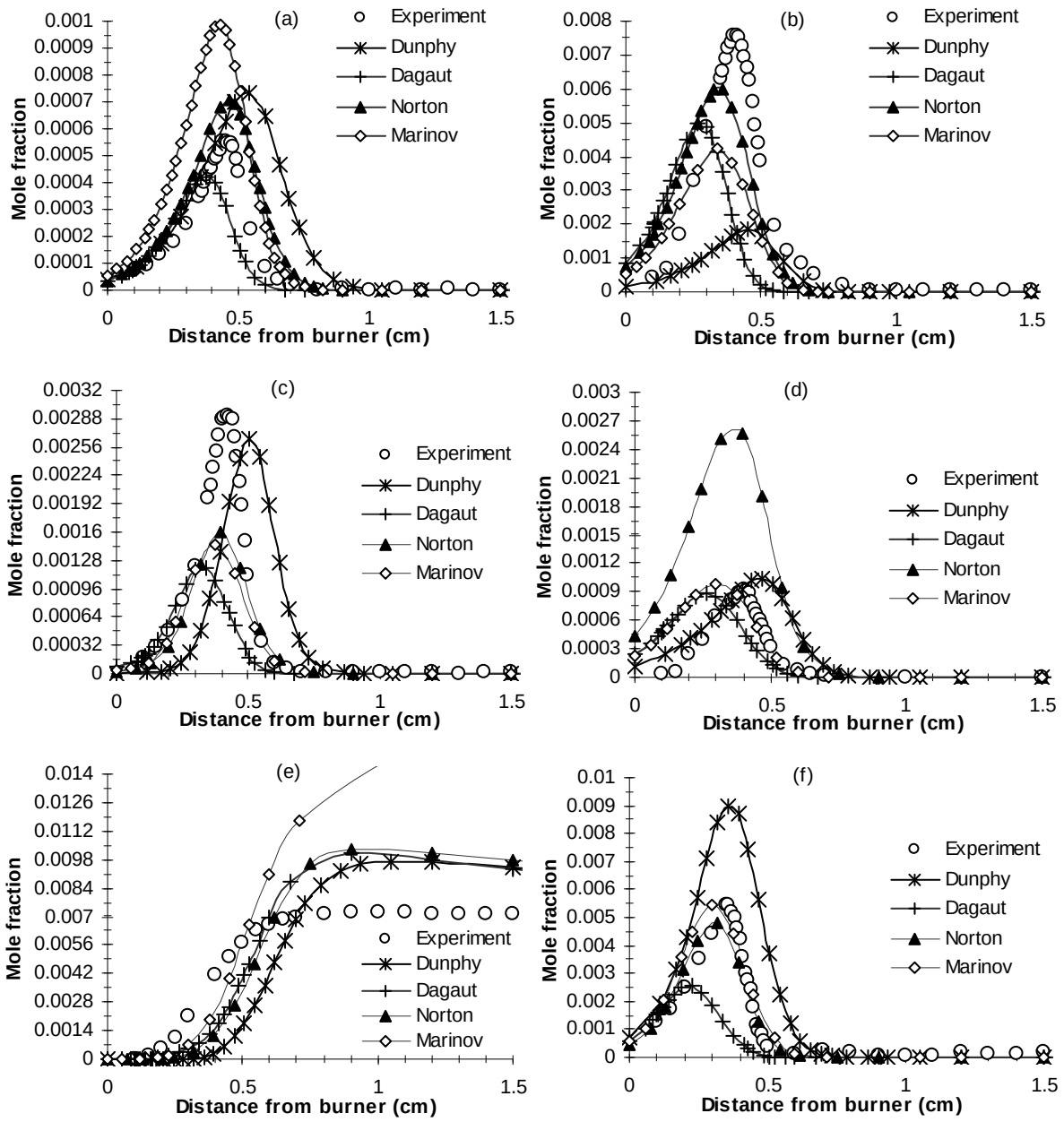

Figure 6 : Experimental and computed mole fraction profiles of intermediate species in a stoichiometric ethanol/oxygen/argon flame : (a) C_2H_2, (b) C_2H_4, (c) $^{\bullet}CH_3$, (d) CH_4, (e) $^{\bullet}OH$ and (f) CH_3CHO.

Table 1 : Flame inlet conditions

	$C_2H_5OH/O_2/Ar$
C_2H_5OH (mole fraction)	0.069
O_2 (mole fraction)	0.206
Ar (mole fraction)	0.725
Equivalence ratios	1
P (mbar)	50
Initial flow velocity (cm/s)	55.7

Table 2 : Characteristics of the modelled mechanisms

Name	Number of reactions	Number of species	Efficiency of third species
Dunphy	97	29	No
Norton	278	32	Yes
Dagaut	76	25	No
Marinov	383	55	Yes

Table 3 : Branching ratios of the ethanol consumption reactions

C_2H_5OH	Norton	Marinov
$+ R^{\bullet} \rightarrow CH_3C^{\bullet}HOH + RH$	49.3 %	37.4 %
$+ R^{\bullet} \rightarrow C^{\bullet}H_2CH_2OH + RH$	26.5%	21.1%
$+ R^{\bullet} \rightarrow CH_3CH_2O^{\bullet} + RH$	17.5 %	41.5 %
$\rightarrow {}^{\bullet}CH_3 + C^{\bullet}H_2OH$	6.8 %	≈ 0 %

Table 4 : percentage of ethanol burning through some intermediate species

Intermediate species	Norton	Marinov
CH_3CHO	49.3 %	58.4 %
C_2H_4	26.5 %	21.1 %
C_2H_2	8.5 %	8.0 %
${}^{\bullet}CH_3$	79.6 %	68.5 %